New Excavations of Middle Stone Age Deposits at Apollo 11 Rockshelter, Namibia: Stratigraphy, Archaeology, Chronology and Past Environments

Ralf Vogelsang, Jürgen Richter, Zenobia Jacobs, Barbara Eichhorn, Veerle Linseele & Richard G. Roberts

Abstract

This paper presents new information obtained from a recent excavation and reassessment of the stratigraphy, chronology, archaeological assemblages and environmental context of the Apollo 11 rockshelter, which contains the longest late Pleistocene and Holocene archaeological sequence in Namibia. The Middle Stone Age (MSA) industries represented at the site include an early MSA, Still Bay, Howieson's Poort and late MSA. Optically stimulated luminescence (OSL) dating of individual quartz grains yielded numerical ages for the Still Bay and Howieson's Poort, and indicated the presence of a post-Howieson's Poort phase. OSL dating also verified conventional and accelerator mass spectrometry radiocarbon ages for a further two later MSA phases. The timing of the transition from the MSA to the early Later Stone Age was also investigated. Improved resolution of the excavation and a more detailed stratigraphy revealed the presence of near-sterile cultural layers, which in some cases assisted in subdividing the MSA cultural phases. Such information, in combination with the new radiocarbon and OSL chronologies, helps address questions about the duration and continuity of MSA occupation at the site. Analyses of the faunal and archaeobotanical remains show some differences between the occupation phases at the site that may be associated with changing environmental conditions.

Résumé

Cet article présente de nouvelles informations issues d´une fouille récente et d´une relecture de la stratigraphie, de la chronologie, des assemblages archéologiques et du contexte environnemental de l´abri sous roche d´Apollo 11. Ce dernier contient la plus longue séquence stratigraphique du Pleistocène supérieur et de l'Holocène en Namibie. Le site a fourni diverses industries du Middle Stone Age (MSA), notamment le MSA inférieur, le Still Bay, le Howieson´s Poort et le MSA supérieur. La datation de grains individuels de quartz, effectuée par luminiscence optique (OSL), a donné les âges absolus des cultures Still Bay et Howieson´s Poort et a aussi montré la présence d´une phase post-Howieson´s Poort. La datation par OSL a également confirmé l'âge attribué à deux phases MSA tardives, anciennement datées par la méthode du radiocarbone. Les étapes de la transition entre le MSA et le Later Stone Age inférieur ont aussi été étudiées d'un point de vue chronologique. La précision apportée à la séquence stratigraphique au cours des nouvelles fouilles a permis d´observer des couches presque stériles, qui permettent parfois de mieux séparer les phases culturelles du MSA. De telles observations, accompagnées de la nouvelle séquence chronologique radiocarbone et OSL, contribuent à la discussion sur la durée et la continuité des occupations du MSA dans le site. Les analyses fauniques et archéobotaniques indiquent quelques différences entre les phases d´occupation humaine du site, peut-être associées aux changements d´environnement naturel.

Keywords: Apollo 11, Still Bay, Howieson's Poort, MSA, early LSA, OSL dating, archaeofauna, palaeoenvironment

Ralf Vogelsang *(corresponding author)* r.vogelsang@uni-koeln.de / **Jürgen Richter**
Universität zu Köln, Institut für Ur- und Frühgeschichte, Forschungsstelle Altsteinzeit, Weyertal 125, 50923 Köln, Germany

Zenobia Jacobs / Richard G. Roberts
Centre for Archaeological Science, School of Earth and Environmental Sciences, University of Wollongong, New South Wales 2522, Australia

Barbara Eichhorn
Goethe-Universität Frankfurt, Institut für Archäologische Wissenschaften, Archäologie & Archäobotanik Afrikas, Grüneburgplatz 1, 60323 Frankfurt a. Main, Germany

Veerle Linseele
Center for Archaeological Sciences, Katholieke Universiteit Leuven, Celestijnenlaan 200E - bus 2409, B-3001 Leuven, Belgium

DOI 10.3213/1612-1651-10170 Published online in October 2010

Study background

The first excavations at Apollo 11 were made by W.E. Wendt in 1969. The rockshelter is known mainly as the site of discovery of Africa's earliest examples of figurative art, which are around 30 thousand years (ka) old. The painted slabs are the earliest-known African paintings (Wendt 1974, 1976), complemented recently by finds in South Africa of decorated ochre pieces at Blombos Cave, dated to 70–100 ka ago (Henshilwood *et al.* 2002; Henshilwood *et al.* 2009), and a similar, but slightly younger, piece from the Howieson's Poort layer at Klein Kliphuis (Mackay & Welz 2008).

Equally important, but less well known than its works of art, Apollo 11 also has one of the most complete Middle Stone Age (MSA) and Later Stone Age (LSA) archaeological sequences in southern Africa. All important cultural units known from the regional MSA and LSA are contained in a single sequence less than 2 m in depth. When Wendt began work at Apollo 11 in 1969, the first excavations at Klasies River had just taken place and there was little general interest in the southern African MSA compared with more intensive research into the LSA and related rock art. Publication of the Klasies River work in 1982 (Singer & Wymer 1982) and the MSA overview by Volman (1984) opened up new perspectives on the southern African MSA, which expanded subsequently following discussion of the "Out of Africa II" hypothesis, which attracted worldwide interest in the development of the MSA in southern Africa.

In subsequent years, significant advances in radiocarbon (^{14}C) dating have been made, including the measurement of ^{14}C by accelerator mass spectrometry. These advances prompted a new dating program at Apollo 11, which was one of the most comprehensively ^{14}C-dated archaeological sequences for its time. However, ^{14}C dating has a practical maximum age limit of around 40 to 50 ka, depending on sample preparation procedures, so alternative numerical dating methods are required for older deposits. Given recent improvements to the accuracy and precision of ages obtainable using optically stimulated luminescence (OSL) methods, we decided to re-excavate a portion of the Apollo 11 sequence to retrieve sediment samples for OSL dating. The combination of OSL and ^{14}C chronologies would permit us to re-evaluate the ages obtained from the entire stratigraphic sequence at Apollo 11, focussing especially on the lower, previously undated, layers beyond the range of ^{14}C methods.

Physical setting

The Apollo 11 rockshelter is located on the eastern slope of the Nuob Rivier, a tributary of the Orange River that flows approximately 40 km further to the south (***Fig. 1***). The Nuob cuts through the western foothills

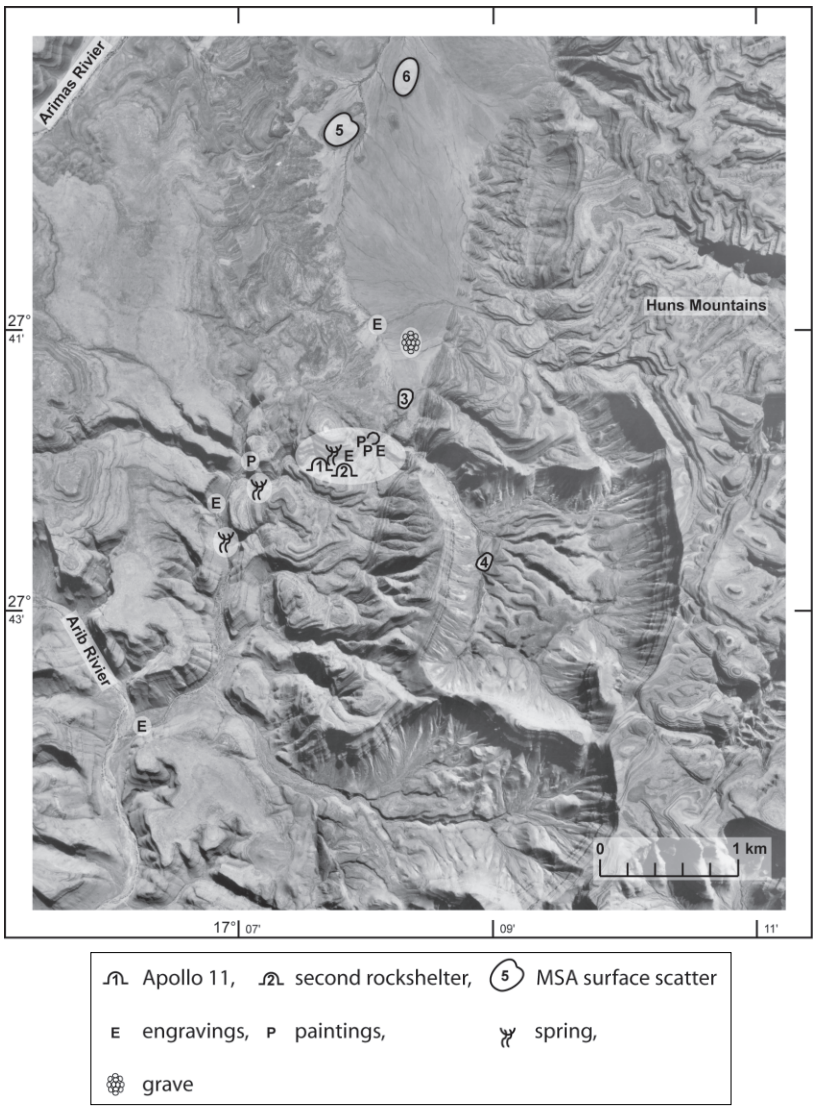

Fig. 1. Location of Apollo 11, MSA surface sites and rock art sites.

Fig. 2. Rock-shelter Apollo 11 upon the Nuob Rivier, Southern Namibia.

of the Huns Mountains, which form the northern part of the Ai-Ais Richtersveld Transfrontier Park. Close to the site, the ephemeral river has cut a gorge 50 m deep into the black limestone, which is assigned to the Huns Member (Martin 1965: 107–110). The carbonates of the Huns Member were originally referred to the Schwarzkalk Limestone by Martin (1965), and were later described in more detail by Germs (1972, 1983). They are now assigned to the southern Witputs sub-basin of the Nama Group (Grotzinger *et al.* 2005: 501), which unconformably overlies the metamorphic rocks of the Namaqualand Metamorphic Complex.

Inclusions of shale and sandstone, in particular, are common in the black limestone, as are quartzite and conglomerate inclusions. The rockshelter has formed as a result of the weathering and erosion of a clayey shale lens in the more resistant limestone. Similar processes of denudation continue to operate today in the vicinity of the site.

The entrance to the rockshelter is 28 m wide and orientated towards the north-west. It is situated 20 m above the valley floor (***Fig. 2***) and extends 11 m from the drip line to the back wall of the shelter (***Fig. 3***). Some large rockfall boulders rest on bedrock at the entrance to the shelter, partially shielding it from the slope below. Sediments have been trapped behind these boulders since the earliest MSA settlement, resulting in comparatively extensive deposits being preserved at this site. Because of the sedimentary infill, a person can stand nearly upright on the present-day floor only in the front section of the rockshelter.

Environment

The south-western corner of Namibia is at present a semi-desert environment, with mean annual precipitation of less than 100 mm. Variation in annual rainfall is very high and, in contrast to all other parts of the country, a significant portion of the rain (10–30 %) falls during the winter months (Mendelsohn *et al.* 2002: 84–89; Stengel & Leser 2004: 130). The low precipitation rates strongly influence the vegetation, which is a Dwarf Shrub Savannah, characterised by low shrubs and grassland, such as Driedoring (*Rhigozum trichotomum*), Black Thorn (*Acacia mellifera*), Stinkbush (*Boscia*

Fig. 3. The 28 metre wide rock-shelter entrance of Apollo 11.

foetida) and Wild Hair Tree (*Parkinsonia africana*). Typical grasses include *Stipagrostis* species, which are resistant to aridity (Müller 1985). Trees are restricted to the dry river beds (*e.g.*, Camel Thorn/*Acacia erioloba*, Sweet Thorn/*Acacia karroo*, Karee/*Rhus lancea*, Laurel Fig/*Ficus ilicina*). In addition to the dwarf shrub vegetation, plants of the Succulent Steppe dominate the surroundings of the rockshelter. As the name suggests, this vegetation type is characterised by succulents. Of particular note is the occurrence of different species of *Aloe* and *Euphorbia*, which grow on the slopes of the mountains and valleys (Giess 1971; Mendelsohn *et al*. 2002: 98–99). The spectrum of "Veldkos" (edible wild plants) is relatively limited: the main potential sources in the vicinity of the rockshelter are Small-leaved Cross-berry (*Grewia tenax*), White Puzzle Bush (*Ehretia alba*) and Natal Plum (*Carissa* sp.) (W.E. Wendt, pers. comm.).

Under the present arid environmental conditions, the only large mammals in the Nuob Rivier are mountain zebra (*Equus zebra hartmannae*), klipspringer (*Oreotragus oreotragus*), rock hyrax (*Procavia capensis*), leopard (*Panthera pardus*) and baboon (*Papio ursinus*).

The low and variable rainfall is the main limiting factor for survival of fauna in the region, thus the deep erosional grooves in the river bed in front of the shelter are of great importance for retaining water during droughts. They are fed by seepage water and commonly hold water even in dry years. A spring known as "Goachanas" is located approximately 2 km from Apollo 11 and provides a permanent supply of water.

History of research

The Apollo 11 rockshelter was originally named "Goachanas" by the rock-art specialist E.R. Scherz, who brought it to the attention of Wendt (Scherz 1986: 376). Despite its relatively large dimensions, however, Apollo 11 yielded only a few rock paintings: a white zigzag-line (partly bordered in red), two handprints, three geometric images and some traces of colour (*ibid.*). Similar drawings are found on several boulders and rock faces in the vicinity of Apollo 11; all of these sites are largely hidden and comprise only a few depictions.

Numerous engravings are found on the smoothly polished, black limestone banks in the valley floor, in front of the shelter. In addition to many relatively unweathered geometrical designs that appear to have been made in the recent past, there are some naturalistic animal depictions (Scherz 1970: 41). These are obviously older, since they display a much heavier patination, and some are only visible under favourable light conditions (***Fig. 4***). Some remarkable fine-line

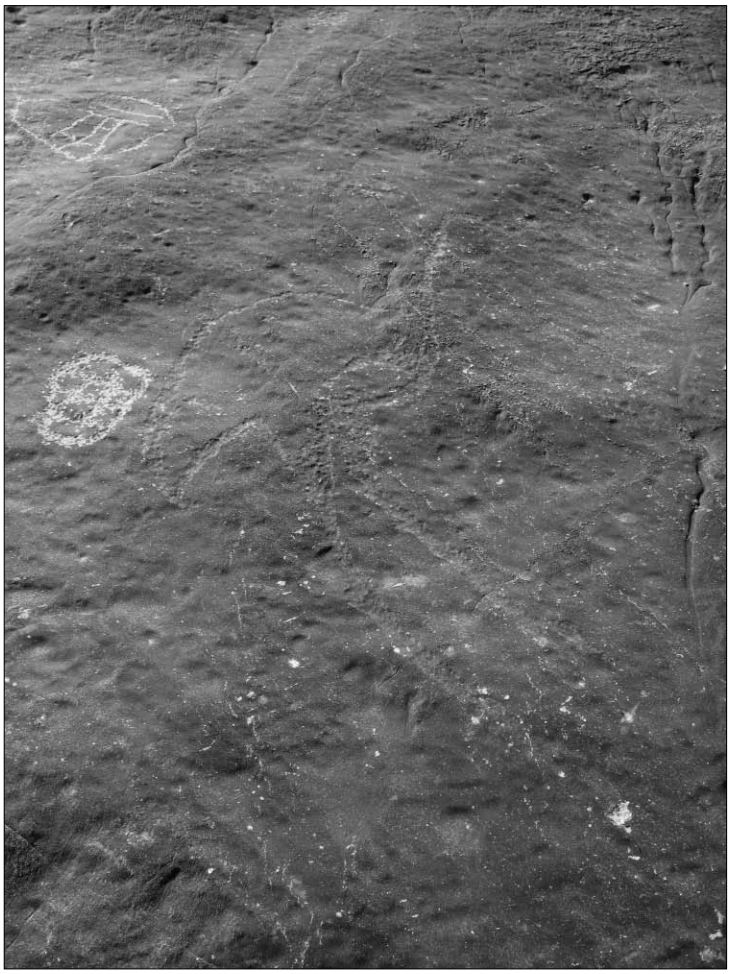

Fig. 4. Engraving of an ostrich in the river bed in front of the rockshelter (size ~ 50 cm).

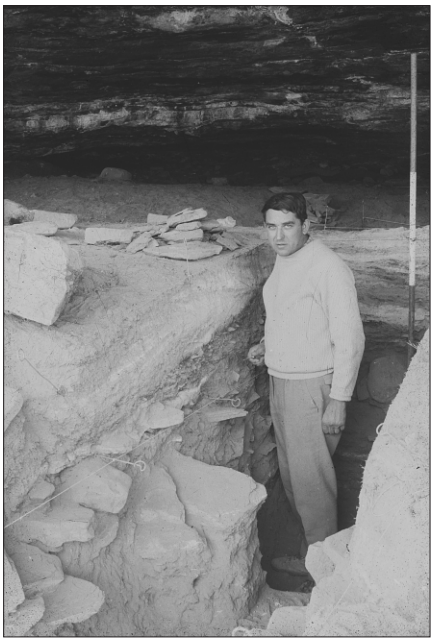

Fig. 5. The excavator Dr. W.E. Wendt during the excavation in 1969 in trench A.

engravings of running antelopes and ostriches, which are stylistically and technologically unusual, occur on a vertical rock face about 400 m from the rockshelter (Vogelsang, personal observation).

Because Goachanas is the name of the spring located 2 km further downstream of the rockshelter, and not of the seepage directly in front, Wendt decided to rename the site. Deeply impressed by the successful return of the spacecraft "Apollo 11" to Earth during his first field season, he decided to name the site after the spacecraft.

Excavations at Apollo 11 commenced in 1969 with a test pit of 2.5 m^2 in area in the north-western corner of the rockshelter, directly beneath the zigzag painting. A large boulder penetrates the surface at this spot, having fallen from the rock face where the painting was later applied. Wendt hoped to determine a terminus post quem for the rock art by dating the cultural layers beneath the boulder, but the deposit was too shallow and the few finds were not informative. He subsequently excavated a second trench, measuring 9.5 x 1 m, near the middle of the shelter (***Fig. 5***). In 1972, he extended this trench by 2.25 m^2, but only for the uppermost MSA layers (Wendt 1974).

The 2007 excavations

In 2007, the old trench was re-opened by a team from the University of Cologne and enlarged by 0.5 m^2, with excavations extending from the surface down to bedrock. The main purpose of this re-excavation was to collect samples for ^{14}C, OSL and electron spin resonance (ESR) dating. When the previous excavations were conducted, ^{14}C dating was the only available means of obtaining numerical ages for the youngest MSA complex and the more recent archaeological deposits (Vogelsang 1998: 95). Since then, numerical dating of more ancient deposits has become feasible with the development of alternative methods, such as OSL and ESR, which have larger time ranges.

In addition, it was hoped that improved excavation methods would allow finer chronological differentiation between the lithic assemblages. During his excavations in 1969 and 1972, Wendt excavated 1-metre squares in spits of varying thickness. In general, the Holocene layers were excavated in 5 cm-deep spits,

but their thickness increased to 10 cm and sometimes up to 20 cm in the MSA layers (Wendt 1974: 6). As a result of this excavation strategy, settlement horizons of different age would have been mixed together; thus classification of the cultural material is limited to a differentiation of "cultural complexes", which include numerous settlement episodes spanning several hundreds, if not thousands, of years (Vogelsang 1998: 40–41). Nevertheless, these cultural complexes differ sufficiently from each other in their characteristic technological and typological attributes to provide some understanding of cultural developments during the MSA. The re-excavation in 2007 was intended to test the potential to distinguish between the cultural layers at Apollo 11 at higher resolution.

Excavation methods

An area of 0.5 m^2 adjacent to the central part of the old trench was chosen for re-excavation. The areas close to the back wall of the shelter and in front of the drip line, both of which are especially prone to disturbances by post-depositional processes, were avoided. In addition, the newly excavated squares were located close to where Wendt had found the painted slabs. The trench was divided into quarter-metre squares and excavated in spits of 5 cm depth; spits were subdivided more finely when visible sediment changes were observed during excavation. Every spit or sub-spit was marked with a "position number". All excavated material was sieved in three stages, using mesh widths of 10, 5 and 2.5 mm. All finds were separated according to material type (stone, pottery, ostrich eggshell, bone, wood, charcoal and other botanical macro-remains) during the excavation process.

Sampling for OSL and ESR dating was done by the relevant dating specialists, who participated in the 2007 excavations.

Stratigraphy

In general, the central and upper parts of the Apollo 11 stratigraphic sequence should be viewed as predominantly anthropogenic in origin, consisting of fireplaces, occupation levels and bedding places, rather than as a sequence of naturally deposited sediments with interfingering cultural layers. Natural sedimentation processes will have dominated over the products of human activity at certain times, the sediments being derived mainly from the roof of the shelter with some input from aeolian sources. The natural accumulation of sediment seems to have exceeded the anthropogenic contribution only in lower layers U–Y and in central layer N (***Fig. 6, Tab. 1***).

Sediment units A–L, comprising the Holocene and terminal Pleistocene deposits, exhibit a heterogeneous and complicated

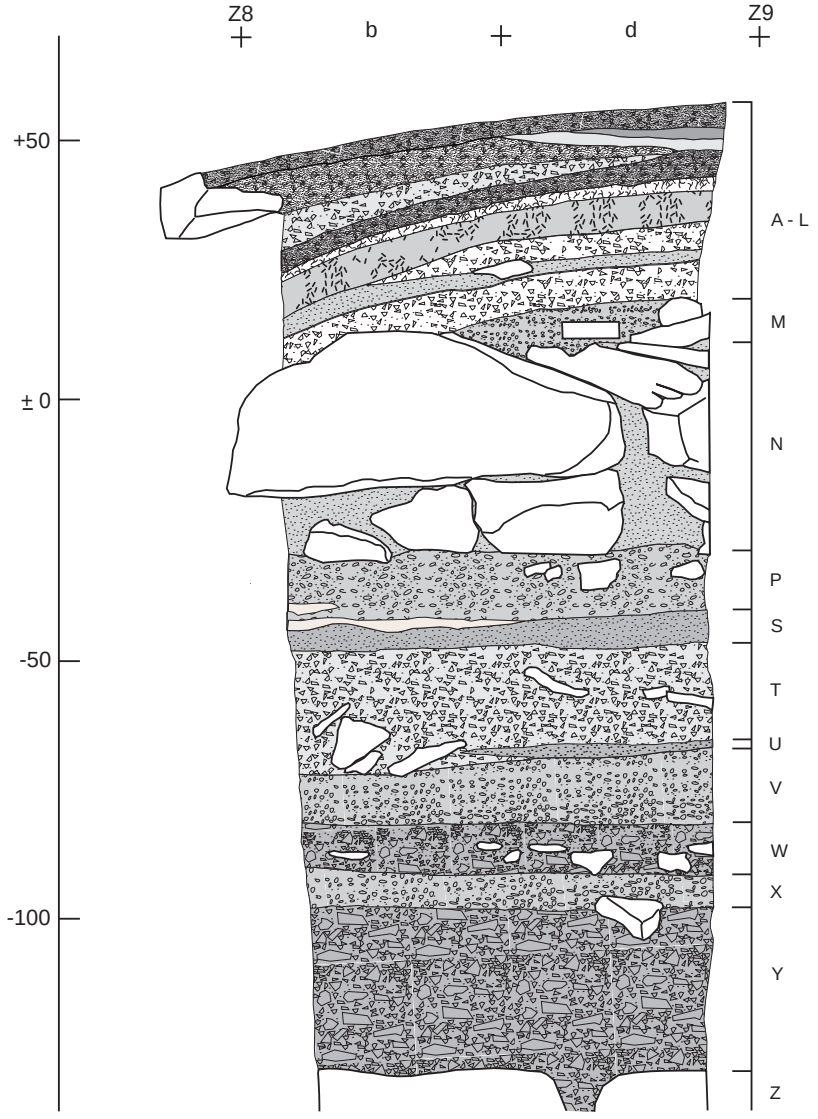

Fig. 6. Schematic stratigraphic drawing, section Z8b – Z9d.

Unit	Description
A	fine-grained heterogeneous, mostly ashy, sediment with some limestone rubble from the roof of the shelter, heavily loosened and disturbed by trampling
B	layer of mixed ash and plant material, consisting mostly of grass. It is presumably a bedding layer (see WADLEY 1979: 23), or the product of several re-deposited beddings
C	homogeneous dark grey ashy lens restricted to the southern half of the section. It has the shape of a wide, shallow pit
D	repeats the shape of unit C, but now consists of homogeneous white ash, probably indicating the remnant of a fireplace. The shallow pit containing sediment units C and D had clearly been established after removal of prior deposits, mainly unit E
E	extends throughout the whole of the section, essentially repeating the homogeneous character of sediment unit B, thus indicating another bedding layer
F	light grey dusty silt, rich in limestone rubble, which might indicate that this unit (like sediment unit A at the surface) was subaerially exposed for a sufficient length of time to allow debris from the roof to accumulate
G	light grey dusty silt, mixed with plant remnants, thus resembling bedding layers B and E
H	multiple bedding layer, the sequence of several plant beddings still clearly visible in superposition
I	grey and brown dusty silt, with some rubble and abundant artefacts and charcoal indicating an occupation surface
J	white ash mixed with fine rubble and thin slabs of limestone
K	thin layer of grey brown dusty silt with a few limestone slabs
L	white ash with fine-grained limestone rubble
M	dusty sediment of brown colour (7.5YR 5/4) interspersed with finely laminated grit layers, indicating continuous weathering of the roof of the shelter
N	densely packed deposit, consisting of boulders with small amounts of silt of a light brownish grey colour (10YR 6/2) filling the interstices. Some of the boulders are very large. Intense weathering and/or tectonic activity are possible explanations for the accumulation of this clast-supported deposit
P	dusty sediment of light olive brown colour (2.5Y 5/3), mixed with fine-grained rubble. In the southern half of the excavation, unit P is in direct contact with underlying unit S
Q	lens of white ash, overlain by sediment unit P
R	ashy lens that is white in the upper part and grey in the lower part. Units Q and R are restricted to the northern half of the excavation
S	homogeneous dusty silt of olive brown colour (2.5Y 4/4) that is packed very loosely
T	consolidated silt of brown colour (7.5YR 4/3), mixed with fine angular debris and some larger slabs in a partly inclined position
U	rounded, calcareous concretions 2–3 mm in size, restricted to the southern half of the excavation
V	homogeneous layer of horizontally laminated, fine rock debris
W	heterogeneous mixture of horizontally laminated, fine to coarse rock debris
X	resembles sediment unit V
Y	resembles sediment unit W, except that the amount and size of rock debris increases towards the base of the unit. Some of the larger rock slabs are in an upright position
Z	large rock boulders, with sediment unit Y filling some of the interstices. Unit Z probably marks the friable weathered surface of the black limestone bedrock, within which the shelter has formed

Tab. 1. Sediment units Apollo 11, squares Z8 and Z9. For technical reasons (that is, the section is interrupted by a step, causing an offset of 0.5 m between the overlying and underlying parts of the section), we omitted the letter "O" from the series and continued the description of the sequence at the letter "P".

stratigraphic sequence. Numerous thin layers of deposit, highly interspersed with organic material (animal dung and botanical remains), alternate with ash lenses including charcoal concentrations and layers containing fine limestone rubble. When "dust" or "dusty silt" is mentioned in ***Table 1***, it refers mainly to ash and probably dissolved dung; when "plant remnants" are mentioned, it refers mostly to stems and grass stalks. The colours of the sediments are different shades of grey (Munsell Soil Colour Chart 7.5YR 3/1, 5/1 and 6/1, 10YR 7/1 and 7/2), and the ash lenses are pale yellow to white (2.5Y 8/2).

The lower layers are more horizontally bedded than are the upper layers, so the depths (in cm) listed in ***Table 2*** are reliable for the lower layers but only approximate for the upper layers. All depth values apply to the situation in squares Z8 and Z9 of the 2007 excavation, and probably to adjacent squares A8 and A9 of Wendt's excavation. Correlation with his sedimentary units ("1969 units" in ***Tab. 2***) is also approximate. The right-hand column in ***Table 2*** shows "groups" of uncalibrated ^{14}C ages for neighbouring samples; ages are shown in parentheses if they fall outside the main groups by more than two standard deviations (95 %

depth cm	1969 units	2007 units	kinds of deposit	predominant agents	cultural horizons 1998	cultural horizons 2009	grouped ^{14}C ages uncal. bp ka
+ 55	V	**A**	surface	*human*	LSA		
+ 50	VII	**B**	bedding	*human*		Final LSA	**0.4 to 0.3**
		C	fireplace	*human*		Ceramic LSA	**1.6 to 1.4**
		D	fireplace	*human*			
+ 45		**E**	bedding	*human*		Micro. LSA I	**6.4 to 6.2**
		F	bedding / ash / dung	*human*/natural		Micro. LSA II	**7.2**
+ 40		**G**	bedding	*human*			
		H	bedding	*human*		Micro. LSA III	**9.4**
+ 35		**I**	buried surface	*human*			
+ 30		**J**	fireplace	*human*/natural			
		K	bedding / ash / dung	*human*	ELSA	ELSA I ELSA II	
+ 20		**L**	fireplace / fine rubble	*human*/natural			**14.5 to 13.0**
+ 10	III	**M**	bedding / ash / dung	*human*			**19.7 to 17.3** (21.6) **28.4 to 25.6**
- 30		**N**	boulder / rubble	catastrophic natural event	MSA 4	Late MSA I Late MSA II Late MSA III	**33.3 to 32.7** **39.8 to 38.5** (46.4)
- 40		**P**	fine rubble / silty sed. bedding / dung	natural/ *human*	MSA 3	gap	*infinite ages*
		Q	fireplace	*human*		Howieson's Poort	
		R	fireplace	*human*			
- 45	II	**S**	bedding / fine rubble	*human*/natural	MSA 2	gap	
- 65		**T**	dung / rubble	*human*/natural		Still Bay	
	I	**U**	fine rubble / calcrete	natural		gap	
- 80		**V**	rubble	natural	MSA 1.2	Early MSA I	
- 90		**W**	rubble	natural			
- 100		**X**	fine rubble	natural		gap	
- 130		**Y**	rubble	natural	MSA 1.1	Early MSA II	
						gap	
- 135	0	**Z**	rubble / bedrock	natural		Early MSA III	

Tab. 2. Stratigraphic units and estimated ages, based on uncalibrated ^{14}C-dating.

confidence interval). The resulting groups of ^{14}C ages indicate 10 periods of human occupation of Apollo 11 between the latest MSA and the final LSA. Three of these ^{14}C age-groups lie within Marine Isotope Stage (MIS) 3, two occur in MIS 2, and the other five age-groups reflect Holocene occupation of the shelter.

The fine-grained rockfall in the lower layers may be attributed to a more humid climate. Over the time period covered by units T to P (Still Bay and Howieson's Poort, both of infinite radiocarbon age), human activities played an increasing role in sedimentation. During the second half of MIS 3, Late MSA occupation coincided with a possible natural catastrophe: a rockfall resulting in boulders falling on to the occupation surface. We speculate that ancient earthquakes may have triggered this rockfall, possibly in association with neotectonic displacements along the Hebron Fault in southwest Namibia, which was active as recently as the late Pleistocene and Holocene (White *et al.* 2009).

After this rockfall event, the climate became increasingly arid in the lead up to the Last Glacial Maximum. The deposit contains scant evidence for extensive weathering and dissolution of the shelter roof under these dry conditions, with anthropogenic activities exerting greater control over sedimentation processes throughout the LSA.

Cultural sequence

The 2007 excavation yielded a total of 648 MSA stone artefacts. The improved excavation strategy (spits of 5 cm depth, or less) permitted artefact densities to be determined at higher resolution than previously and this allowed for a finer division of the stone artefact assemblages (see below, "Continuity and gaps"). On the whole, the general trends of the previous analysis (Vogelsang 1998) are consistent with the new data set and complemented by the additional detail provided by the latter. It seems justified and expedient, therefore, to maximise the sample size for this paper by combining the archaeological data obtained from the 1969, 1972 and 2007 excavations at Apollo 11.

Originally, in the publication of the MSA material from Wendt's excavation (Vogelsang 1998) the adoption of the southern African terminology for the cultural phases from Namibian MSA inventories was avoided. The only exception was the Howieson's Poort, because in this case the conformity was very obvious. Other terms, for example the Still Bay, were less clearly defined and the assignment to Namibian inventories seemed to be an oversimplification. Instead, a sequence of numbered phases was compiled for each site. Corresponding phases were combined to cultural groups in the conclusion, using a new Namibian terminology, but following Volman's MSA phases for Southern Africa (Vogelsang 1998: tab. 1, 250–253). However, this approach holds the risk of causing confusion and misunderstanding and is therefore abandoned in this paper in favour of a more generalized Southern African terminology.

Late MSA (previously Apollo 11 MSA 4 [Vogelsang 1998])

The excavations undertaken by Wendt in 1969 and 1972 (Wendt 1972, 1974, 1976) yielded a total of 21,265 MSA stone artefacts (excluding chips < 1 cm). Of these, 2678 (12.6 %) can be classified to the late MSA. In contrast to all older MSA complexes, quartz (mostly in the form of pebbles) plays an important role in the stone artefact raw material spectrum, comprising 11 % of the total late MSA assemblage. Due to its unfavourable fracture quality, most quartz is inappropriate for the production of very regular flakes and blades, but regularity was apparently not a critical criterion. Most flakes from the late MSA inventory are, in general, irregularly shaped, even though more suitable quartzite and calcareous mudstone dominate the raw material spectrum. Blades are relatively rare and the proportion of angular debris is high. Cores are rarely prepared and most have been exploited in an opportunistic way; regular core types are very rare. The informal character of the inventory is also reflected in the comparatively unstandardised length dimensions of the complete flakes and blades. The number of retouched tools is very low (1.1 %), and it is the absence of specific tool types that characterises this inventory. There is only one retouched point, for example, and two doubtful fragments. Backed pieces, which are numerous in the underlying Howieson's Poort layers, are also represented only by sporadic finds. The classification of this inventory as a MSA assemblage, therefore, is based solely on the presence of typical unmodified blanks as pointed flakes and blades.

A special mention should be made of one stone artefact from this cultural unit: a blade bearing traces of resinous mastic at the base. Most probably, this blade had been hafted in a handle made of organic material and was used as a knife. The use of adhesives to haft stone tools is known from Howieson's Poort and post-Howieson's Poort inventories from Sibudu Cave (Lombard 2006, 2008). Ochre as an ingredient of the adhesive, detected in these inventories, is not proven for the Apollo 11 specimen.

Among the numerous ostrich eggshell fragments (n = 4481; 3375 g), 22 pieces with specific fractures on their inside surfaces are noteworthy (***Fig. 7.2***). Experiments suggest the deliberate opening of the eggshells by picking with a pointed stone flake (Vogelsang 1998: 236–238). The reconstructed diameters of the apertures correspond with those of ostrich eggshell flasks, which are known in southern Africa from the LSA to the recent past (*e.g.*, Morris 1994; Henderson 2002). Although carnivores feeding on ostrich eggshells may produce confusingly similar marks (Kandel 2004), we consider it more likely within the cultural context of Apollo 11 that the modified pieces can be interpreted as ostrich eggshell flask apertures.

Seven fragments show traces of red colouration that may indicate ornamental painting of ostrich eggshell as early as the late MSA (***Fig. 7.3***). Unfortunately, these pieces are too small to be definitive about the origin of the red traces: they may be remnants of decoration, but could equally originate from spilled flask contents.

The most spectacular artefacts of the latest MSA complex at Apollo 11 are the painted slabs. Radiocarbon dating of charcoal from the immediate proximity of the slabs indicated an age of about 27,500 ^{14}C years before present (Wendt 1974, 1976). These depictions are not only the oldest drawings known from the African continent, but are also some of the earliest pieces of evidence for artistic creation anywhere in the world. The

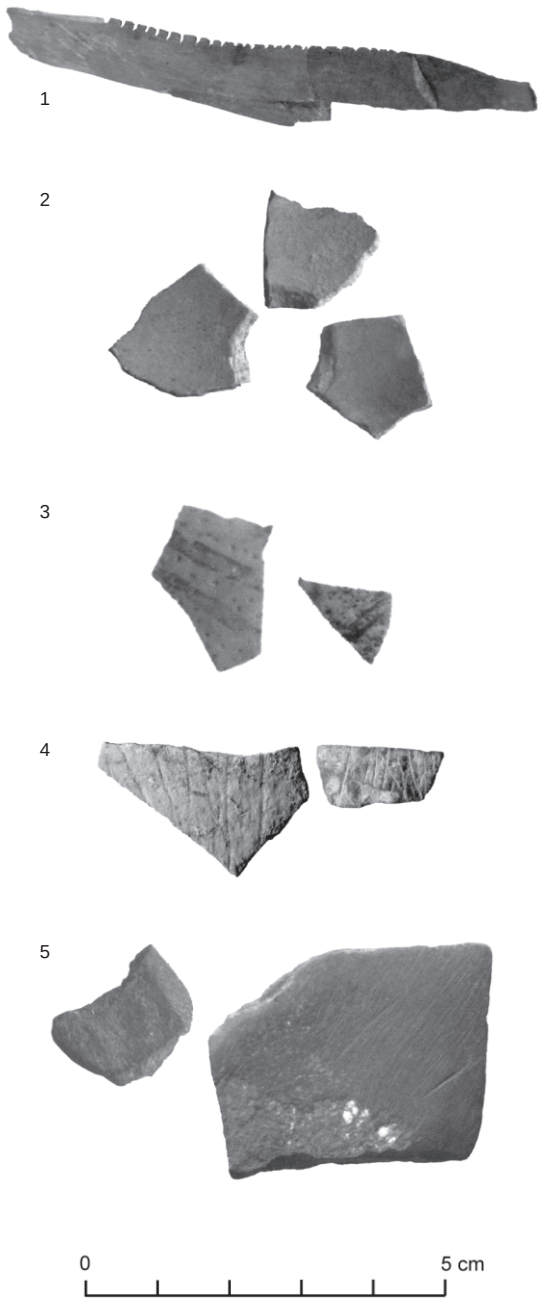

Fig. 7. Extraordinary artefacts: a notched rib fragment (1), fragments of ostrich eggshell flasks apertures (2), ostrich eggshell fragments with traces of red colour and incisions respectively (3, 4), pigment schist with clear traces of abrasion (5).

stone slabs consist of different varieties of clay schist that outcrop in the vicinity of the shelter. The seven fragments are not exfoliated parts of a larger wall painting, but are separate representations on loose slabs ("art mobilier"). This conclusion is based on the different schist varieties of the slabs, the central position of the representation on the only complete slab, and the concentration of these finds in only 2 m^2 of Wendt's original excavations. Furthermore, one drawing was applied to the cleavage face of the slab and was, therefore, certainly made after the slab had separated from the rock face.

In contrast to rock paintings of the LSA, the depictions were not made by applying liquid paint to the rock with a brush or fingers, but by drawing with a "pigment crayon". A large variety of pigmented schist, exhibiting a broad spectrum of colours, can be found in the gravels of the Nuob Rivier, and three of the drawings combine different colours. With the exception of the drawing of a rhinoceros, the zoological identification of the representations is ambiguous. One slab, consisting of two fragments, shows the body of an animal, most likely a feline, with human hind legs that were probably added subsequently (***Fig. 8***). Two barely visible lines at the head resemble Oryx horns, and a lappet at the abdomen may represent the sexual organ of a bovid. Indeed, it may depict a supernatural creature, a so-called "therianthrope", which would suggest a complex belief system.

Terminal MSA/post-Howieson's Poort assemblages (MSA 3 assemblages according to Volman's classification scheme) are comparatively rare in southern Africa. Furthermore, their typological and technological characteristics are not uniform across this region (Volman 1984; Mitchell 2002: 85–86, 111; Willoughby 2007: 282). The late MSA from Apollo 11 is archaeologically significant, therefore, as one of the few known occurrences of the geographically widespread post-Howieson's Poort.

Howieson's Poort (previously Apollo 11 MSA 3 [Vogelsang 1998])

The underlying MSA 3 complex corresponds to the Howieson's Poort, as described by Volman (1984: 203–204), Thackeray (1992: 390) and Wurz (2002: 1009–1010). It yielded 10,876 stone artefacts (Vogelsang 1996, 1998: 79–80), amounting to 51.1 % of the total number excavated by Wendt. This is the highest number of stone artefacts of any of the MSA complexes at Apollo 11, despite the relatively small volume of corresponding deposit.

The Howieson's Poort at Apollo 11 differs in most aspects of stone artefact technology from the preceding (Still Bay) and following (late MSA) complexes. Calcareous mudstone (49.1 %) dominates the raw material spectrum, followed by quartzite (26.8 %) and a comparatively high proportion of cryptocrystalline silicates (15.4 %). The latter were apparently preferred for their excellent knapping suitability, which is crucial for the production of relatively small segments and allied forms.

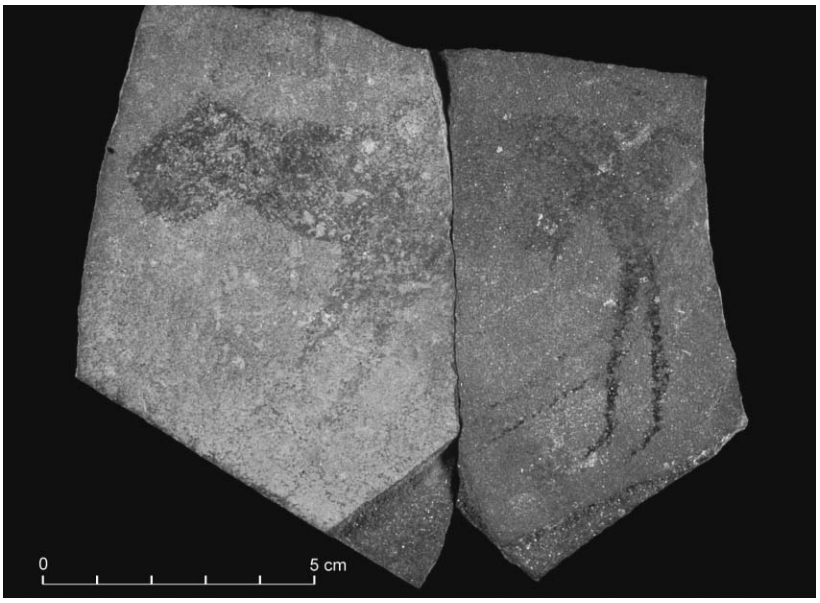

Fig. 8. Depiction of a "therianthrope" combining a feline body, human hind legs and Oryx horns.

The high proportion of flakes (55.3 %) and a higher proportion of angular debris (14.0 %) distinguishes the stone artefact material from the underlying assemblages, owing to its somewhat "crude" appearance. The proportion of blades (29.1 %) is smaller than in all older complexes, and the small fraction of complete blades (28.0 % of all blades) suggests intentional breakage. The proportion of distal and proximal fragments is comparable (***Fig. 9.1–3, 9.10*** and ***9.11***). By contrast, medial fragments are relatively rare, although their short length indicates multiple breakages (***Fig. 9.4–9***). The size of medial fragments seems to be standardised and they are rarely retouched, but their edges commonly show signs of abrasion (64 %). It appears that unretouched medial blade fragments were systematically produced during the Howieson's Poort and used for special tasks outside the shelter, which would explain their low numbers in the assemblage. The length distribution of complete flakes shows a comparable standardisation: they are very short, having a mean value of 1.95 cm and a maximum of 3 cm, so the size of the raw material nodules would not have been critical. Demand for high-quality raw material was met by long-distance transport of "exotic" rocks and intensification in the use of pebbles, in particular of cryptocrystalline silicates, from the dry river beds. The high number of cores, predominantly small in size, compared to the older assemblages, and the increased proportion of cortex flakes (34 %), supports the proposition that mostly small nodules and pebbles were brought complete to the rockshelter for further core preparation and débitage production.

The fraction of retouched artefacts (7.1 %) in the Howieson's Poort complex is higher than in all of the other assemblages. Backed pieces are common (20.5 %) and the numerous truncations are mainly steep. The Howieson's Poort has the highest number of different tool types of all MSA assemblages from Apollo 11. All type forms of the previous complexes are represented, but points with retouched edges are less numerous. Tool types exclusive to the Howieson's Poort include large segments (> 2.5 cm, n = 11; ***Fig. 9.18–24***), straight backed blades (n = 33; ***Fig. 9.15–17***) and convex backed blades (n = 45; ***Fig. 9.25–28***). In addition, 35 pieces have a steep truncation (***Fig. 9.12–14***), which is a feature also of the underlying Still Bay assemblage. Typical core types are single-platform cores, cores with two opposite platforms, and discoidal cores. The continued appearance of characteristic Still Bay tool types, such as bifacially and unifacially retouched points (n = 3 and n = 10, respectively; ***Fig. 9.29*** and ***9.30***) contrasts with the otherwise considerable changes in stone tool technology and contradicts the impression of the Howie-son's Poort being a foreign intrusion in the otherwise continuous MSA cultural sequence.

The 4081 ostrich eggshell pieces in the Howieson's Poort levels have a total mass of 3312 g and are mainly unworked fragments. Potential ostrich eggshell flask apertures are represented by 23 pieces. Exceptional finds include two small fragments with intentionally carved lines on the outside (***Fig. 7.4***) and three pieces with smoothed edges, comparable to LSA ostrich eggshell pendants. The size of all fragments is too small, however, for an unambiguous attribution.

Also noteworthy is the unusually high number of mineral crystals (n = 90) found in the Howieson's Poort layer, especially calc-spar, although it is not clear why they were collected.

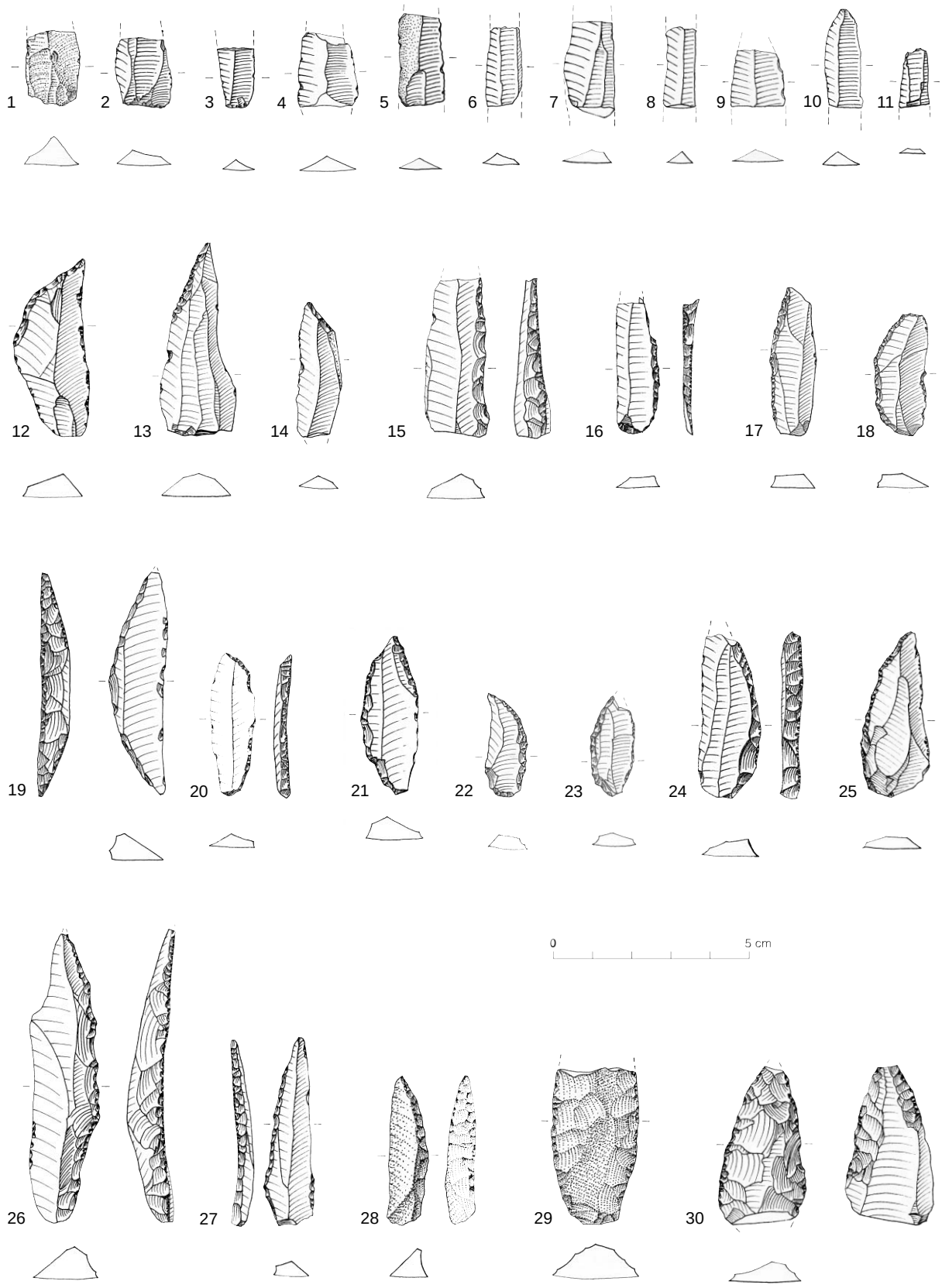

Fig. 9. Howieson's Poort stone artefacts: Blade fragments (1–11), truncated pieces (12–14), straight backed blades (15–17), large segments (18–24), convex backed blades (25–28), bifacial point (29), unifacial point (30).

Still Bay (previously Apollo 11 MSA 2 [Vogelsang 1998])

Beneath the Howieson's Poort, and separated by a thin sterile layer, is a stone artefact complex that shares affinities with Still Bay assemblages from South Africa. However, definitive criteria for classification of a stone artefact assemblage as "Still Bay" are still quite vague, so the term is used here with reservations. Indeed, the definition of Still Bay bifacial points used by Villa *et al.* (2009) to describe large samples from the South African sites of Blombos, Sibudu and Diepkloof calls the classification of the Apollo 11 specimens into question. In particular, the only two complete pieces from Apollo 11 are less elongated than the typical Still Bay points.

The Still Bay contains 5521 stone artefacts (26.0 % of the total for the entire MSA). In contrast to all other MSA assemblages, quartzite (52.4 %) replaces calcareous mudstone (34.0 %) as the prevalent raw material. The quartzite is predominantly of a fine-grained variety that outcrops locally, including an exposure in a dry river bed close to the shelter. This variety is ideally suited to the production of very regular blades, which characterise the débitage production (***Fig. 10.16–19***). The manufacture of standardised forms is reflected in the high proportion of blades and blade fragments (42.4 %), the low proportion of angular debris (12.8 %), and the preference for regularly-shaped flakes (quadrangular and triangular; ***Fig. 10.7*** and ***10.8***). The linear dimensions of complete blades and flakes show a differentiation into two size ranges.

The proportion of retouched tools (6.8 %) is only slightly lower than in the Howieson's Poort assemblage. Crudely and finely retouched edges dominate (51.7 % and 30.1 %, respectively), whereas backed retouch is rare; two backed pieces might be intrusive from the overlying layer. Facial retouch is characteristic of the Still Bay, and typical stone tool type forms in this unit include bifacial points (n = 4; ***Fig. 10.1, 10.11*** and ***10.12***), unifacial points (n = 14; ***Fig. 10.2–6***) and edge-retouched points (n = 13; ***Fig. 10.9*** and ***10.10***). Of special interest are "basal end scrapers on pointed blades" (n = 7; ***Fig. 10.13–15***), which appear in Still Bay inventories at other Namibian sites also (Pockenbank, Aar 1; Vogelsang 1998: 102, 122), thereby justifying their designation as a type form. Characteristic regular core types are single-platform cores, cores with two opposed platforms, and Levallois cores.

Ostrich eggshell is well preserved (7000 fragments, 3720 g), but many pieces, especially from the rear of the shelter, have scorch marks. The Still Bay layer contains the oldest evidence of pieces with specific fractures, which may indicate the use of ostrich eggshell flasks (Vogelsang 1998: 235–238). There is no indication of any other modification of ostrich eggshell.

Except for the area in front of the drip line, bones are comparatively well preserved, even in the MSA layers. But in contrast to the existing LSA bone points and awls at Apollo 11 and evidence from other MSA sites in southern Africa (*e.g.*, Blombos Cave: Henshilwood *et al.* 2001; d'Errico & Henshilwood 2007, Sibudu Cave: Backwell *et al.* 2008), no artefacts were made of this raw material during the MSA. The only exceptions are two rib fragments with notches, which were recovered from the Still Bay layer (***Fig. 7.1***). The larger piece (7.2 cm in length) has 23 regular, fine notches at one longitudinal edge; the other piece (6.2 cm in length) has 12 slightly less regular notches. In all probability, a third notched piece collected from sediment that collapsed from the profile can be assigned to the Still Bay layer. In all cases, the possibility that these are cut-marks from de-boning can be ruled out, but it is unclear if the notches are merely decorative or if they bear a functional meaning.

The Still Bay inventory provides the earliest proof for the collection of minerals at Apollo 11. In addition to pieces without any obvious function, such as rock crystal, quartz crystal and calcite, two larger pieces of haematite were used as pigments. More numerous are schistose, ochreous pigments (n = 35) that are present in abundance in the dry river bed in front of the rockshelter. Three of these show clear abrasion marks, indicating their use as crayons or to produce pigment powder (***Fig. 7.5***).

An unusual feature of the Still Bay layer is a concentration of larger blocks of stone that are loosely piled up. These stones originate from the valley slope and not as rock debris from the shelter wall. The pile of stones has a maximum width of 1.8 m and a height of 0.5 m, but a regular structure is not discernible, at least in the small area exposed by excavation. Charcoal and burned plant remains are concentrated in this area, but none of the stones shows any impact from heat. The stones may have formed the base of a hut structure, given their proximity to the rear wall of the shelter (about 2 m away), but a sound interpretation requires the excavation trench be enlarged.

Early MSA (previously Apollo 11 MSA 1 [Vogelsang 1998])

The basal deposits (unit V–Z) differ from the other layers in that the charcoal, plant remains, bone and ostrich eggshell are less well preserved. This may indicate a substantial time gap between the early MSA and the

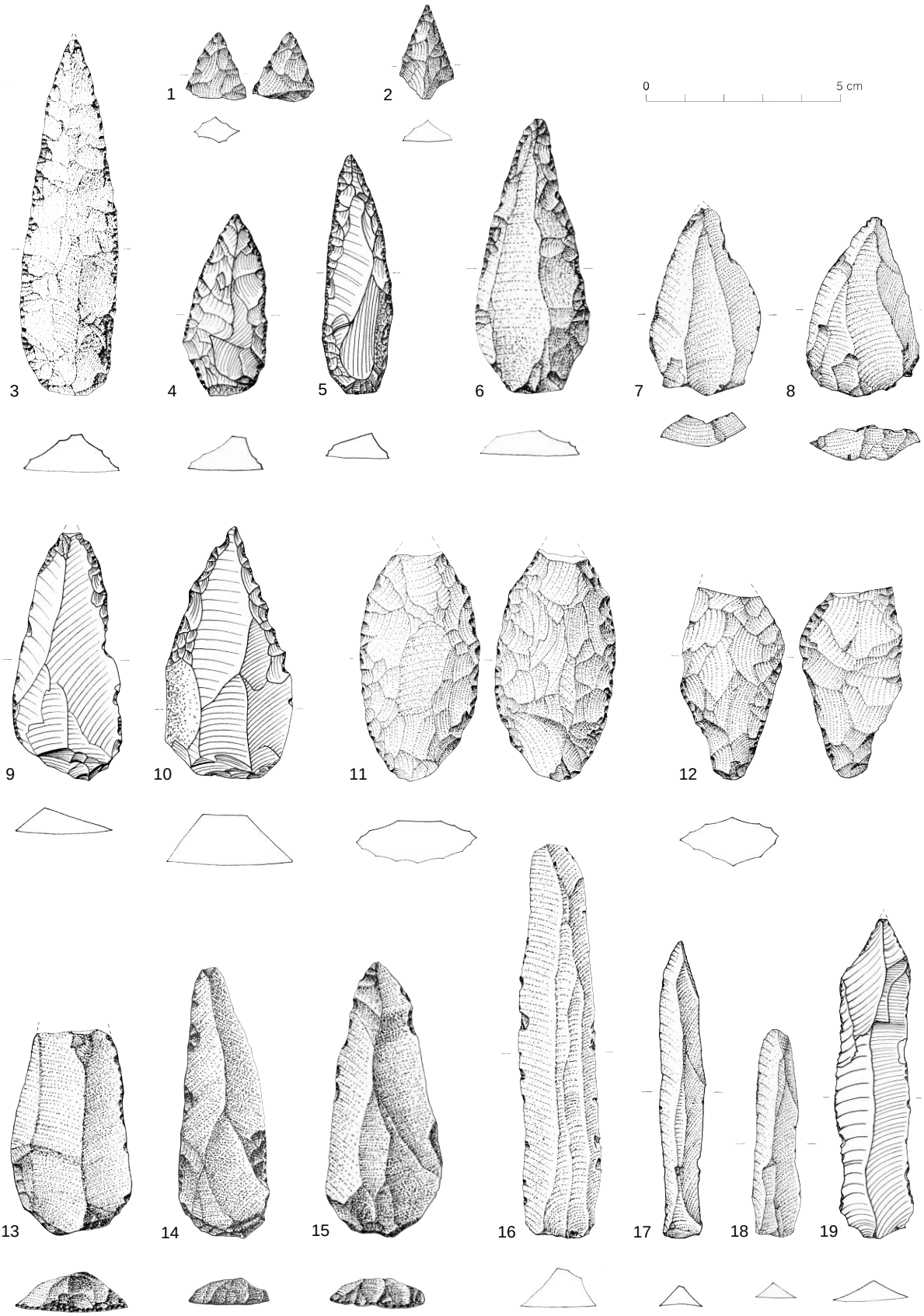

Fig. 10. Still Bay stone artefacts: bifacial points (1, 11, 12), unifacial points (2–6), pointed flakes (7, 8), edge-retouched points (9, 10), basal end scrapers on pointed blades (13–15), blades (16–19).

Still Bay. The difference is underlined by a clear change in the character of the sediments, which contain a large amount of fine to coarse rock debris in the basal layers; the proportion of the coarse fraction generally increases with depth.

Despite the overall uniformity of the stone artefacts, especially the technological aspects, the early MSA layer was subdivided into two phases (phase 1 and phase 2 of Vogelsang 1998: 68–73) to account for changes in the distribution of artefacts and types of stone tools. In the following, the two early MSA phases are compared and contrasted, to emphasise their many similarities on the one hand and their distinguishing features on the other.

The boundary between the lower phase 1 and the overlying (younger) phase 2 runs approximately through the middle of the basal deposit, but phase 1 contains twice as many stone artefacts (n = 1475) as phase 2 (n = 715). The stone artefacts in phases 1 and 2 were made almost exclusively from quartzite (48.4 % and 48.0 %, respectively) and calcareous mudstone (42.7 % and 39.2 %, respectively). These raw materials occur locally in large quantities, and would need to have been available in sufficient quantity and size during the early MSA to manufacture the prevalent large flakes and blades. We attribute the low number of cores, and the low proportion of flakes with cortex, in the early MSA layers at Apollo 11 to core preparation and débitage production being conducted largely at factory sites next to the rock outcrops.

Blades and blade-like flakes are a common feature of early MSA phases 1 and 2 (31.2 % and 30.6 %, respectively), but the mode of production appears to have been somewhat unsophisticated. The artefact shapes are, in most cases, irregular and there is a smooth transition between blades senso stricto and blade-like flakes. Complete pieces of both débitage types also exhibit a wide variation in their linear dimensions.

Few artefacts in phases 1 and 2 are intentionally retouched (4.2 % and 5.5 %, respectively), but the majority have edge damage (52.3 % and 51.1 %, respectively). At least some of these may be interpreted as use-wear, but the role of post-depositional processes must also be taken into consideration.

During phase 1, the main types of retouch are coarse and fine edge retouch (44.8 % and 37.9 %, respectively), with denticulated retouch in a minority of cases (13.8 %; ***Fig. 11.4–6***). During phase 2, coarse edge retouch clearly dominates (58.0 %) and facial retouch (6.5 %) appears for the first time. Only a few formal tool types can be recognised in phase 1. Characteristic types include coarsely retouched side scrapers, denticulated blades, notched pieces (***Fig. 11.1***) and truncated flakes. Coarsely retouched edge scrapers are absent from phase 2. An edge-retouched point and a unifacial retouched point in the early MSA assemblages may represent the oldest examples of these tool types at Apollo 11, or they may have intruded from the overlying Still Bay layer, where both types are common. By contrast, unmodified pointed flakes are prevalent in the early MSA assemblages (***Fig. 11.9–12***).

As mentioned above, preservation of ostrich eggshell is comparatively poor during the early MSA. Pieces are quite small and highly fragmented (phase 1: n = 447; 500 g, phase 2: n = 337; 350 g), only a few show burn marks, and none has been modified intentionally.

Whereas no pigments can be assigned unambiguously to phase 2, 14 pieces were recovered from the phase 1 layers. Pigment shale dominates the collection, and can be found in high quantities in the dry river bed in front of the shelter, but there are also some brittle examples in unusual tones. None of the pigments, however, shows any traces of use-wear.

Continuity and gaps

One of the main reasons for re-excavating Apollo 11 in 2007 was to use improved excavation methods (*i.e.*, smaller excavation units and more detailed section drawings) to allow a better chronological differentiation of the lithic assemblages. The benefits of this excavation strategy were confirmed by new results for the density distribution of artefacts and by a more finely resolved stratigraphy of the shelter deposits.

Based on the material collected during the 1969 and 1972 excavations, the distribution of artefacts was interpreted as indicating more or less continuous settlement of the rockshelter. While there must have been several long-lasting settlement gaps, which were verified by the absence of ^{14}C ages for some periods in the younger layers, they could not be detected by searching for spits with considerably fewer finds. This impression of apparent continuity can be shown to be erroneous, on the basis of the density distribution of artefacts recovered from the smaller excavation units in 2007.

From the new excavations, it is apparent that some phases have very low artefact densities and, hence, no clear indication of human settlement activity. The absence of such layers in Wendt's excavation is, at least partly, a consequence of the relatively crude excavation method employed at that time, amplified by the

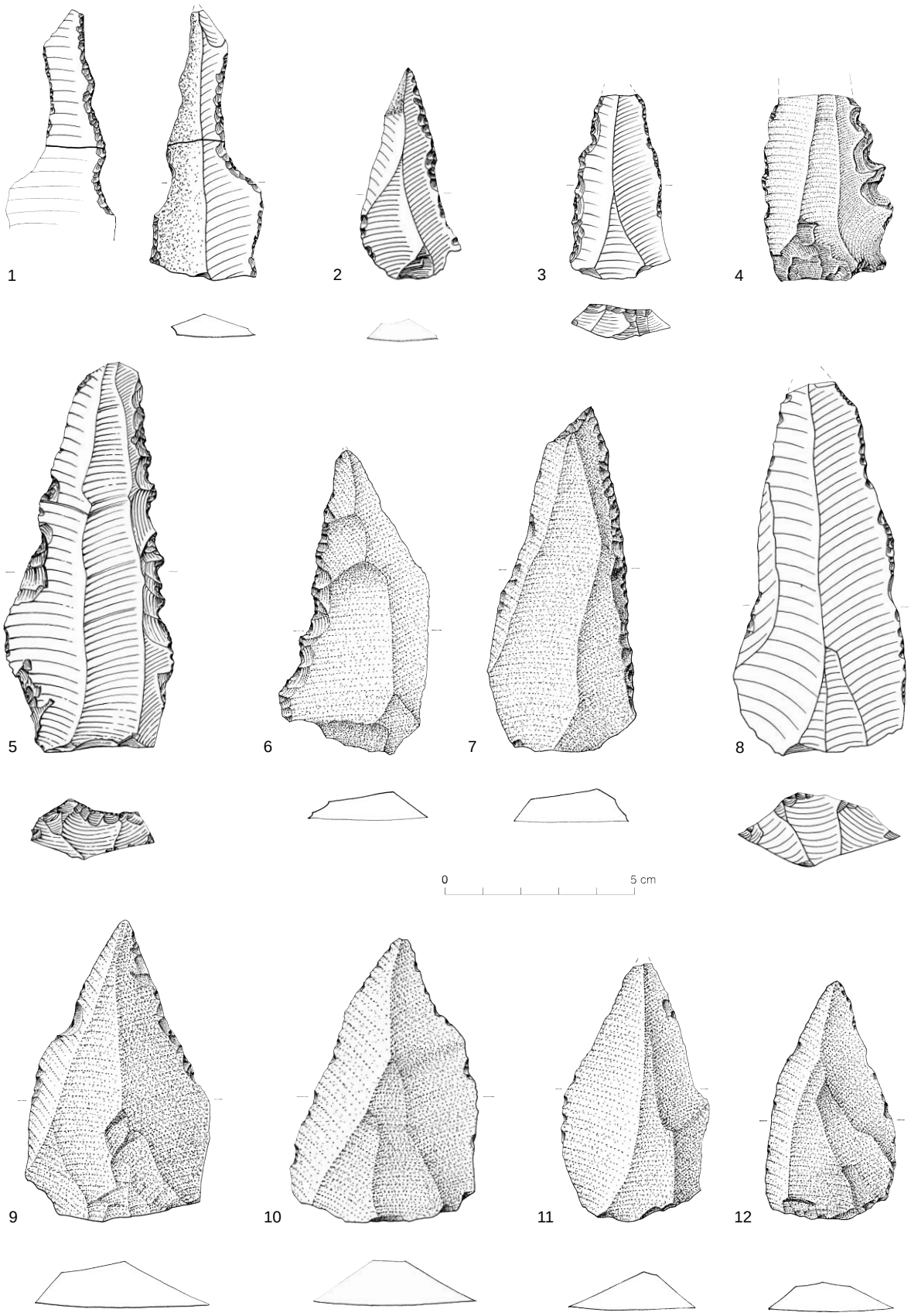

Fig. 11. Early MSA stone artefacts: notched piece (1), retouched points (2, 3), denticulated pieces (4–6), blades (7, 8), pointed flakes (9–12).

low rates of natural sedimentation in the shelter (*cf.* Vogelsang 1998: 44–45).

Thin, near-sterile layers confirm that some cultural complexes are separated by gaps in occupation, as described above, such as the Still Bay and Howieson's Poort complexes (***Tab. 1, Fig. 6***). In other instances, the near-sterile layers suggest a subdivision of cultural complexes. Particularly evident is the subdivision of the basal early MSA complex into phases 1 and 2, and the hiatus between the early MSA and Still Bay complexes. Most commonly, the excavation units with low artefact densities correspond to thin layers of silty sediment and/or very fine rock debris, which may reflect increased aeolian sedimentation under extremely arid conditions. The 1969 and 1972 section drawings, made mainly at a scale of 1:20, did not reveal these layers, which seem to be characteristic of settlement gaps.

These new results emphasize the great potential of the Apollo 11 deposit to yield a refined chronology for the MSA cultural complexes, and they provide a compelling reason to consider the site for future excavations.

Dating

In the following dating sections we have adopted a slightly modified nomenclature for the cultural complexes to enable the finer chronological divisions to be distinguished. For ease of comparison, both sets of terms are shown in ***Table 2***.

Radiocarbon dating

When the Apollo 11 artefact assemblages were first analysed in the late 1970s, conventional ^{14}C dating was the only appropriate means of obtaining numerical ages for the types of material collected for dating. Depending on the method of sample preparation, ^{14}C dating has a maximum reliable age limit of 40–50 ka, which is too young to capture most of the MSA layers at Apollo 11. Numerical age estimates could only be obtained, therefore, for the LSA deposits and the more recent part of the late MSA complex; ***Table 3*** presents details of all the ^{14}C age estimates, expressed in both radiocarbon years before present (bp, where the 'present' is AD 1950) and in calendar years, using CalPal09 (CalCurve: CalPal 2007 Hulu, Weninger & Jöris 2008) to perform the calibration. To facilitate comparison with calendar-year ages produced by other numerical dating methods, such as OSL dating, the ^{14}C ages reported below are expressed in thousands of calendar years before present (cal ka BP).

A total of 44 samples were dated from the original excavations, including nine from the late MSA complex. Detailed descriptions of each sample, and the sample preparation and measurement procedures, are given in Freundlich *et al.* (1980) and Vogel & Visser (1981). Special emphasis was placed on collecting samples for dating from the vicinity of the painted slabs found in the uppermost MSA (MSA 4 in Vogelsang 1998, late MSA I in ***Tab. 2*** and ***3***). Eight of the nine age estimates for the late MSA complex were significantly older than those associated with the earliest LSA, the sole exception being sample Pta-1032. The lowermost LSA (early LSA II in ***Tab. 2*** and ***3***, ***Fig. 12***) has a weighted mean age of 22.3 ± 0.4 cal ka BP, whereas the uppermost MSA (late MSA I in ***Tab. 2*** and ***3***, ***Fig. 12***) has a weighted mean age of 29.8 ± 1.1 cal ka BP. The underlying excavation units, associated with late MSA II and III, yielded ages of ~37 cal ka BP and ~43 cal ka BP, respectively, raising the prospect of three occupation phases in the late MSA complex, separated by two gaps of a few millennia each.

Conventional ^{14}C dating, however, requires large amounts of sample material, typically on the order of ~12 g of charcoal, ~30 g of ostrich eggshell and ~200 g of bone. To meet this requirement, samples had to be collected from entire spits, entailing the risk that the composite samples consisted of mixtures of different age materials. A subdivision of the spits was only possible in exceptional circumstances, where clear sedimentological changes could be observed; such was the case with sample KN-4068 from the late MSA I (30.5 ± 0.8 cal ka BP) and KN-4067 from the early LSA II (20.9 ± 0.2 cal ka BP). In other instances, samples were interpreted as being mixed, such as sample KN-1847, which was collected from the contact zone between the late MSA and the Still Bay and yielded an uncalibrated age of 46,400 $^{+3500}/_{-2500}$ bp (Vogelsang 1998: 90).

To overcome the potential problem of dating mixed-age materials, and to check the validity of the conventional ^{14}C ages for the youngest of the MSA levels, the ^{14}C contents of five new charcoal samples collected from the 2007 excavation were measured by accelerator mass spectrometry (AMS) at the Leibniz Laboratory for Radiometric Dating and Stable Isotope Research, University of Kiel. Substantially smaller amounts of material can be analysed by AMS, so individual pieces of charcoal, rather than aggregates, could be dated. Three of these samples were collected from the early LSA I levels (KIA35914: 15.7 ± 0.2 cal ka BP; KIA35915: 15.5 ± 0.1 cal ka BP; KIA35916: 17.4 ± 0.1 cal ka BP), one was taken from the uppermost MSA (late MSA I), where the painted slabs were found (KIA35917: 29.0 ± 0.4 cal ka BP), and the remaining sample was associated with late MSA III, deeper in the sequence (KIA55918: 42.3 ± 0.4 cal ka BP).

Lab. Number	Excavation unit (depth to datum point)	Cultural complex	Sample material	Date bp	cal BP (68% probability, CalPal09)	δ13
Pta-1009	B3/-12	Final LSA	concentration of charcoal	320 ± 40	400 ± 60	-25.8
KN-1608	B8/+55	Final LSA	concentration of charcoal	490 ± 45	540 ± 30	
KN-1846	B8-9/+50	Ceramic LSA	bedding of uncharred twigs & grass	1460 ± 55	1370 ± 50	
KN-1870	A8x$_2$/+45	Ceramic LSA	scattered uncharred twigs & grass	1670 ± 55	1590 ± 80	
Pta-1918	A8x$_1$/+35	Ceramic LSA	scattered twigs	1960 ± 45	1920 ± 50	-24.8
KN-1609	A7/+35	microlithic LSA	concentration of charcoal lumps	6200 ± 65	7100 ± 90	
Pta-1019	B9/+40	microlithic LSA	concentration of charcoal	6480 ± 80	7390 ± 70	-24.8
KN-1867	A7/+20	microlithic LSA	charcoal lumps from ashy lens	7200 ± 75	8040 ± 80	
Pta-1020	A7/+20	microlithic LSA	scattered charcoal	7280 ± 80	8100 ± 80	-23.5
KN-1610	A7/+10	microlithic LSA	scattered charcoal fragments	9430 ± 90	10750 ± 190	
KN-1611	A7/±0	microlithic LSA	charcoal lumps from ashy lens	9430 ± 90	10750 ± 190	
Pta-1021	A8x$_2$/+25	Early LSA I	scattered charcoal	12500 ± 120	14870 ± 240	-23.7
KIA35915	Z8a/+10	Early LSA I	charcoal	12900 ± 50	15480 ± 60	-24.94
Pta-1010	A8x$_2$/+15	Early LSA I	concentration of charcoal	13000 ± 120	15820 ± 330	-24.5
KIA35914	Z8a/+15	Early LSA I	charcoal lump	13010 ± 70	15700 ± 180	-27.38
KN-1614	A8/+22	Early LSA I	charcoal lumps from ashy lens	13030 ± 100	15850 ± 300	
KN-1811	A7/-4(?)	Early LSA I	charcoal lumps from ashy lens	13470 ± 125	16590 ± 250	
KN-1612	A7/-16	Early LSA I	nest with uncharred twigs	13690 ± 120	16910 ± 90	
KIA35916	Z8/±0	Early LSA I	charcoal lump	14230 ± 55	17410 ± 130	-24.00
KN-1613	A7/-16	Early LSA I	charcoal lumps from ashy lens	14550 ± 60	17770 ± 40	
KN-4067	B9/+13	Early LSA II	charcoal	17380 ± 160	20870 ± 210	-20.76
Pta-1039	A8x$_2$/-2	Early LSA II	uncharred twigs & fine plant remains	18500 ± 200	22160 ± 330	-19.5
KN-4042	B8/-2	Early LSA II	charcoal	18650 ± 170	22410 ± 250	
KN-2057	A9x$_2$/+12	Early LSA II	scattered charcoal fragments & uncharred twigs	18660 ± 210	22380 ± 340	
KN-1812	A7/-28	Early LSA II	scattered charcoal lumps	19760 ± 175	23640 ± 170	
Pta-1032	A8x$_2$/-15	Late MSA I	twigs	21600 ± 300	25780 ± 500	-22.3
KIA35917	Z8/-10	Late MSA I	charcoal lump	24150 ± 150	29030 ± 350	-24.06
KN-4068	B9/+13	Late MSA I	charcoal	25600 ± 800	30500 ± 760	-21.38
Pta-1040	A8x$_2$/-5	Late MSA I	1 piece of charred wood	26300 ± 400	31100 ± 420	-10.1
KN-1813	A9x$_2$/+5	Late MSA I	uncharred twigs, leaves & grass	26700 ± 650	31330 ± 580	
KN-2056	A9x$_1$/±0	Late MSA I	scattered charcoal fragments & uncharred twigs	28400 ± 450	32900 ± 500	
KN-4069		Late MSA II	charcoal	32000 ± 1200	36620 ± 1510	-22.31
KN-2115	A8x$_2$/-10	Late MSA II	scattered uncharred twigs & grass	32700 ± 860	37190 ± 1210	
KN-1869	A9x$_2$/±0	Late MSA II	uncharred twigs & grass	33370 ± 550	37960 ± 1270	
KIA55918	Z8/-20	Late MSA III	charcoal lump	38560 ± 450	42710 ± 390	-12.07
Pta-1041	A9x$_2$/±0	Late MSA III	twigs	39800 ± 1700	43780 ± 1240	-20.3
KN-1847	A9x$_2$/-6	Late MSA/Still Bay (mixed sample)	uncharred twigs	46400 $^{/-2500}_{+3500}$		
KN-1616	A9/-20	Howieson's Poort	charcoal lumps from ashy lens	>48000		
Pta1415	B3/-123	Howieson's Poort	ostrich eggshell	>48400		-2.4
KN-1615	A10/-10	Still Bay	bedding of charred twigs & grass	>49000		
KN-1617	A9/-46	Still Bay	concentration of charcoal lumps	>48500		
KN-1618	A9/-62	Still Bay	charcoal lumps from ashy lens	>48500		
KN-1620	A11/-26	Still Bay	concentration of charcoal lumps	>49500		
KN-1622	A11-12/-30	Still Bay	concentration of charcoal fragments	>47500		
KN-1623	A12/-5W	Still Bay	bedding of charred grass	>48500		
Pta-507	A10/-10	Still Bay	ostrich eggshell	>49000		-5.1
Pta-505	A11/-31	Still Bay	ostrich eggshell	>50500		-5.9
KN-1619	A10/-63	Early MSA	concentration of charcoal lumps	>49500		
KN-1621	A11/-58	Early MSA	concentration of charcoal lumps	>49500		

Tab. 3. Apollo 11 ^{14}C dates.

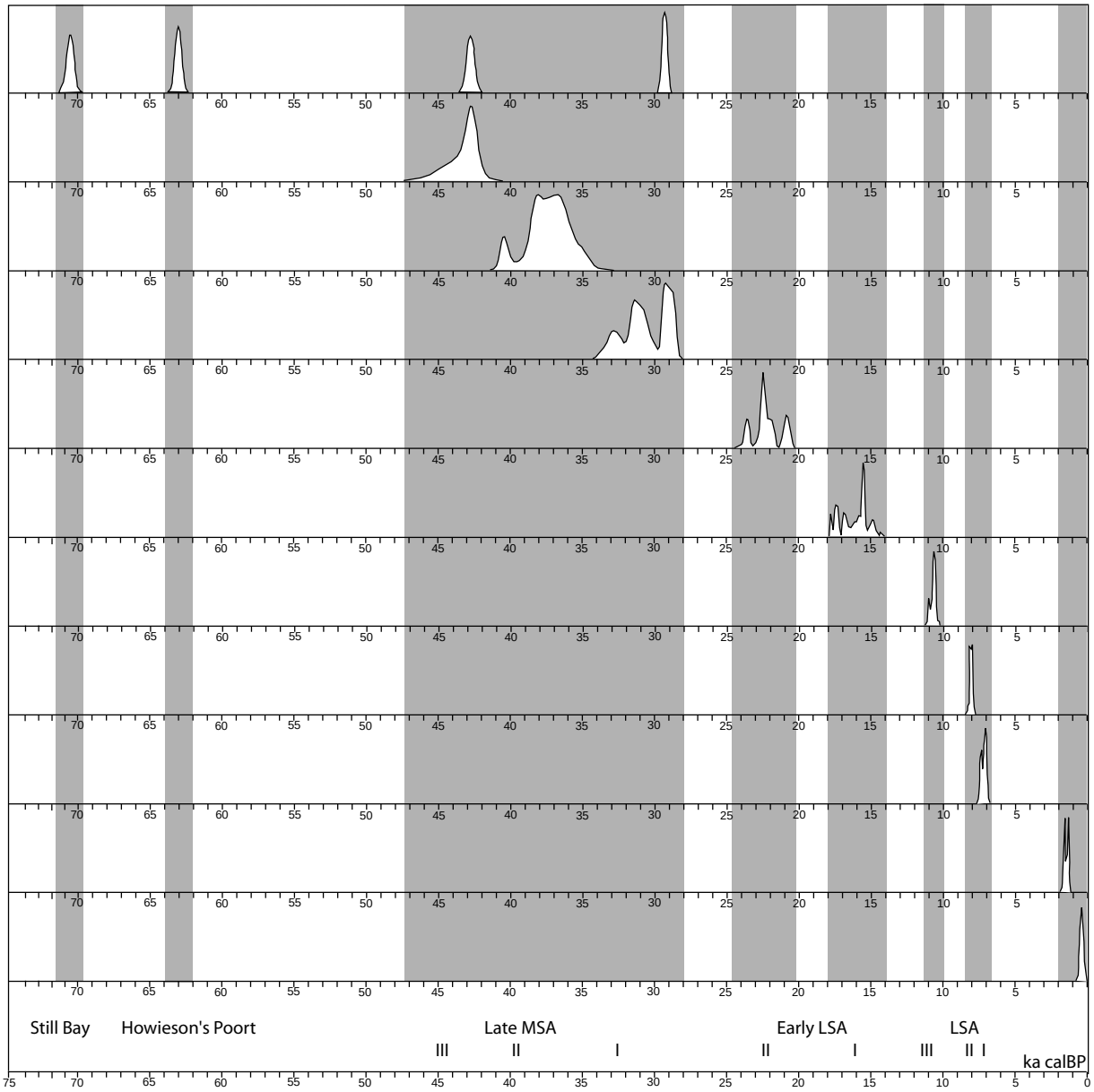

Fig. 12. Apollo 11 settlement phases dated by ^{14}C and OSL (top row).

The new age determinations for early LSA I are consistent with previous, conventional ^{14}C ages for this cultural complex. They are several millennia younger than the ages of ~22 cal ka BP for the lowermost LSA (early LSA II), but as the latter were obtained from large, composite samples, we cannot dismiss the possibility that material from the latest MSA may have been incorporated into the earliest LSA. The conventional and AMS ^{14}C ages for each of the late MSA III and I deposits are statistically concordant and confirm at least two pulses of occupation, at ~43 and ~30 cal ka BP, respectively. The conventional ^{14}C ages for the intermediate late MSA II suggest a third pulse at ~37 cal ka BP. Based on the correct stratigraphic ordering of these ages, mixing within the late MSA complex can be discounted.

An important priority for future excavations and artefact analysis will be to compare changes in artefacts with pulses in occupation during the late MSA.

The greatest limitation thus far has been the inability to obtain finite, numerical age estimates for the earlier MSA deposits. These deposits lie beyond the range of ^{14}C dating, as indicated by a dozen 'infinite' ages (*i.e.*, ages older than 48,000 bp) for various materials (***Tab. 3***). In view of the possibility of mixing in the lowermost LSA levels, and the obtainment of infi-

Sample Code	Moisture content (%)	Dose rates (Gy/ka)			Total dose rate[d,e]	D_e (Gy)[f]	Age model	Number of grains[g]	σ_d (%)[h]	Optical age (ka)[i]
		Beta[a]	Gamma[b]	Cosmic[c]						
Early LSA II & Late MSA I										
AP1	3 ± 1	1.41 ±0.05	0.87 ± 0.04	0.04	2.35 ± 0.09	64.9 ± 0.9	CAM	386 / 1000	19 ± 1	27.6 ± 1.3
						53.1 ± 2.0	FMM			22.6 ± 1.3
						70.9 ± 1.9	FMM			30.1 ± 1.6
Late MSA I										
AP11	3 ± 1	1.34 ± 0.04	0.82 ± 0.04	0.04	2.24 ± 0.09	65.9 ± 1.3	CAM	198 / 1000	14 ± 2	29.4 ± 1.4
Late MSA III										
AP2	3 ± 1	1.38 ± 0.04	0.82 ± 0.04	0.04	2.28 ± 0.09	97.7 ± 4.3	CAM	44 / 900	16 ± 4	42.9 ± 2.7
Post-Howieson's Poort										
AP3	3 ± 1	1.34 ± 0.04	0.82 ± 0.04	0.04	2.23 ± 0.09	131.8 ± 2.5	FMM	192 / 1000	32 ± 2	57.0 ± 2.7
				0.04	2.85 ± 0.06	165.0 ± 6.2	CAM	49 / 500	5 ± 8	57.9 ± 2.6
Howieson's Poort										
AP4	3 ± 1	1.67 ± 0.03	0.91 ± 0.05	0.04	2.65 ± 0.06	167.6 ± 3.5	CAM	201 / 1000	17 ± 2	63.2 ± 2.3
Pre-Howieson's Poort										
AP5	3 ± 1	1.90 ± 0.04	0.92 ± 0.05	0.04	2.89 ± 0.06	193.7 ± 4.8	CAM	64 / 500	6 ± 5	66.9 ± 2.6
Still Bay										
AP6	3 ± 1	1.60 ± 0.03	1.12 ± 0.06	0.04	2.80 ± 0.07	197.7 ± 3.4	CAM	150 / 1000	16 ± 2	70.7 ± 2.6

[a] Measurements made on sub-samples of dried, homogenised and powdered samples by GM-25-5 beta counting. Dry dose rates calculated from these activities were adjusted for the water content (expressed as % of dry mass of sample).
[b] Measurements made using *in situ* gamma spectrometry. Wet dose rates measured were adjusted for the water content (expressed as % of dry mass of sample).
[c] Cosmic dose rates have been calculated using the equations provided by Prescott & Hutton (1994) taking into account the latitude (-27.7°S), longitude (17.1°E) and altitude (1050 m). We have also accounted for the different densities of the overlying roof thickness (2.0 g/cm^3; limestone and sandstone) and sediment (2.0 g/cm^3) and for the cos^2 Φ-zenith angle dependence (see Smith *et al.* 1997). Dry dose rates calculated were also adjusted for the water content (expressed as % dry mass of sample) (see Readhead 1987).
[d] Mean ± total uncertainty (68 % confidence interval), calculated as the quadratic sum of the random and systematic uncertainties.
[e] Includes an assumed internal alpha dose rate of 0.03 ± 0.01 Gy/ka.
[f] Estimated using single grains of quartz. Preheat and cutheat conditions are given in the text.
[g] Number of individual grains used for D_e determination / total number of grains analysed.
[h] Overdispersion (σ_d), the relative standard deviation of the D_e distribution after allowing for measurement uncertainties (Galbraith *et al*. 1999).
[i] The total uncertainty includes a systematic component of ± 2% associated with laboratory beta-source calibration.

Tab. 4. Dose rate data, D_e values and optical ages for 8 sediment samples from Apollo 11.

nite ^{14}C ages for the deposits underlying the late MSA complex, single-grain OSL dating of the sediments at Apollo 11 was carried out.

Single-grain OSL dating

OSL dating provides an estimate of the time elapsed since luminescence minerals, such as quartz, were last exposed to sunlight (Lian & Roberts 2006; Jacobs & Roberts 2007; Wintle 2008). Buried grains will accumulate the effects of the ionising radiation flux to which they are exposed to a distance of ~50 cm, and the stored energy can be measured using the OSL signal to obtain an estimate of the equivalent dose (D_e), which is expressed in grays (Gy). The burial age of grains that were well bleached by sunlight at the time of deposition can then be calculated from the D_e divided by the dose rate due to ionising radiation (***Tab. 4***). OSL ages are obtained in calendar years, and can thus be compared directly with the calibrated ^{14}C age estimates presented in ***Table 3***.

D_e and dose rate determination

We applied single-grain OSL dating procedures to eight samples collected from Apollo 11 (seven from the MSA and one from the LSA); three samples were collected from the eastern face of square A8 and five samples from the northern face of square A9 (***Fig. 13***). All samples were collected in dim red torch-light beneath an opaque (black) tarpaulin. Section faces were first cleaned to remove any grains exposed to sunlight during excavation and sediments for OSL dating were then collected using a trowel to scrape material from the unit of interest into black plastic bags. This approach was taken, instead of hammering plastic or steel tubes into the cleaned section, because of the small depth interval of some of the units/layers of interest and because of the presence of large stones in the deposit.

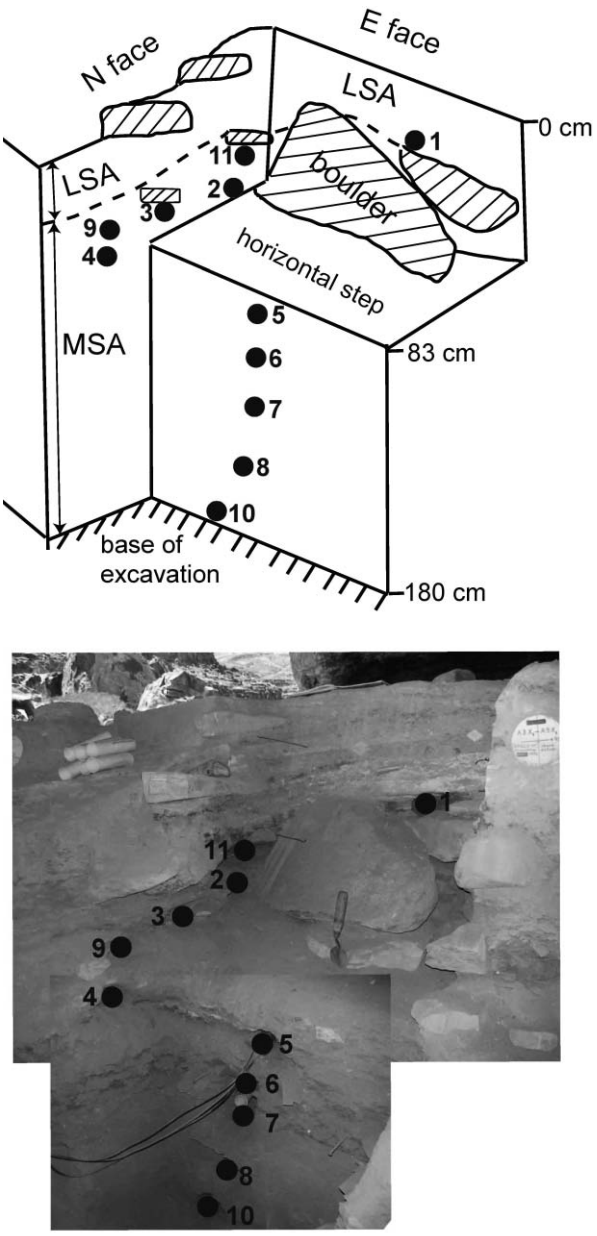

Fig. 13. Location of collected OSL samples.

Quartz grains of 180–212 µm in diameter were extracted from the sediment samples in the laboratory under dim red illumination using standard procedures, including etching by hydrofluoric acid to remove the external, alpha-dosed layer (Aitken 1998; Jacobs *et al.* 2008a). D_e values were obtained from individual grains, to eliminate those with unsuitable OSL properties before calculating the age, and to address concerns about the extent of pre-depositional sunlight exposure and any post-depositional sediment mixing (Jacobs & Roberts 2007). The latter also enables a direct check to be made on the stratigraphic integrity of the archaeological sequence, which is particularly valuable at Apollo 11 because of the possibility of mixing the lowermost LSA with the uppermost MSA deposits, as noted above.

A total of 6900 grains were measured using the single-aliquot regenerative-dose (SAR) protocol, statistical models and experimental instrumentation described elsewhere (Jacobs *et al.* 2006b). Grains were optically stimulated by an intense beam of green (532 nm) laser light (Bøtter-Jensen *et al.* 2003) and the ultraviolet OSL emissions were detected using an Electron Tubes Ltd 9635Q photomultiplier tube fitted with 7.5 mm of Hoya U-340 filter. Laboratory doses were given using a calibrated $^{90}Sr/^{90}Y$ beta source mounted on the OSL stimulation and detection instrument.

After measurement of the natural OSL signal, each grain was subjected to six regenerative-dose cycles and the induced OSL signals were measured. These cycles included a repeat dose and a zero dose, which form part of the SAR protocol performance tests that are routinely carried out on quartz grains (Jacobs & Roberts 2007). After measurement of the natural dose and each regenerative dose, a fixed test dose of ~9 Gy was given and then optically stimulated; the resulting OSL signal was used to monitor and correct for any sensitivity changes between successive SAR cycles. The natural, regenerative and test doses were preheated at 160°C for 10 s before optical stimulation for 2 s at 125°C (at 90 % laser power). The OSL signal was determined from the first 0.22 s of stimulation and the count rate over the final 0.33 s was used as background. At the end of this SAR sequence, a check was also made for the presence of infrared-sensitive grains and inclusions, using the procedure described by Jacobs *et al.* (2003).

As reported in previous studies, not every grain yields useful information on absorbed dose (Jacobs & Roberts 2007). Accordingly, we rejected uninformative grains (***Tab. 5***) using criteria described and tested elsewhere (Jacobs *et al.* 2003, 2006a). For grains that were accepted, a saturating-exponential-plus-linear curve was fitted to the regenerative-dose points and the D_e was obtained from interpolation of the natural signal. Under the measurement conditions specified above, this procedure gave correct estimates of dose for multi-grain aliquots and single grains of sample AP9 (mean ratios of measured/given dose of 1.02 ± 0.04 (n = 6) and 1.05 ± 0.06 (n = 83), respectively) that had been bleached in sunlight and then given a known dose.

The dose rate for each sample is dominated by the beta and gamma dose rates due to ^{238}U, ^{235}U, ^{232}Th (and their decay products) and ^{40}K, making allowance for beta-dose attenuation (Mejdahl 1979) and sample water content (Aitken 1985). The bulk beta and gamma dose rates

Sample	AP1	AP11	AP2	AP3	AP9	AP4	AP5	AP6
				Total number of grains measured				
	1000	1000	900	1000	500	1000	500	1000
				Grains rejected for the following reasons				
T_N signal <3xBG	231	632	753	395	358	246	279	398
0 Gy dose >5% of L_N	2	1	0	1	3	5	6	13
Poor recycling ratio	209	81	43	199	48	141	64	197
No L_N/T_N intersection	103	55	44	163	27	358	73	176
Depletion by IR	69	33	17	50	15	49	14	66
				Sum of rejected grains				
	614	802	857	808	451	799	436	850
				Acceptable individual D_e values				
	386	198	43	192	49	201	64	150

Tab. 5. The number of single grains that were measured, rejected after being subjected to the rejection criteria proposed by Jacobs *et al.* (2003, 2006b) and accepted for inclusion in the calculation of the combined D_e estimate for age calculation.

for each sample were measured by GM-25-5 beta counting (Bøtter-Jensen & Mejdahl 1988) and in situ gamma-ray spectrometry, respectively. The cosmic-ray dose rates were calculated following Prescott & Hutton (1994), and adjusted for the $\cos^2\Phi$ zenith angle dependence (Smith *et al.* 1997) and for water content (Readhead 1987). We assumed an effective internal alpha dose rate of 0.03 ± 0.01 Gy/ka, based on measurements made previously on quartz grains from southern Africa (Jacobs *et al.* 2003).

A water content of 3 ± 1 % was used to determine the OSL age for each sample. This value represents the assumed long-term water content (*i.e.*, averaged over the entire period of sample burial), with an uncertainty sufficient to accommodate the likely range of water contents experienced by the sediments since deposition, including the values measured when the samples were collected; the OSL ages increase by ~1 % for each 1 % increase in water content. We assumed that a condition of secular equilibrium in the U and Th decay chains prevailed throughout the burial period of each sample, and note that the dose rate exhibits only modest variation down the profile: values range from ~2.2 to ~2.9 Gy/ka, with the highest dose rates restricted to deposits underlying the late MSA complex.

D_e distributions and OSL ages

Of the 6900 individual sand-sized grains of quartz measured, between 5 % and 39 % of grains per sample proved suitable for OSL dating using the SAR protocol (***Tab. 4*** and ***5***). The D_e values for these grains are displayed on radial plots in ***Figure 14***. Each point represents a single grain, for which the D_e can be read by extending a line from the "standardised estimate" axis on the left-hand side to intersect the radial axis on the right; the point of intersection is the D_e. The uncertainty on this estimate can be read by extending a line vertically from the data point to intersect the horizontal axis running along the bottom of the plot. This axis shows the relative standard error in % (*i.e.*, the standard error divided by the D_e estimate, multiplied by 100) and its reciprocal (the "precision"). In such plots, the most precise estimates fall to the right and the least precise to the left. If the D_e values were consistent with statistical expectations, then 95 % of the points should scatter within any chosen band of width ± 2 units projecting from the left-hand axis. The width of the ± 2 band is shaded grey in each of the plots in ***Figure 14***. Further information on radial plots is given in Galbraith *et al.* (1999).

For two of the analysed samples (AP5 and AP9), a single grey band can accommodate ~95 % of the points. But for the remaining six samples, some extra spread can be seen in the data. This extra spread is typical for single-grain D_e data sets and is known as "overdispersion"; it represents the spread in D_e values remaining after all sources of measurement error have been taken into account (Roberts *et al.* 2000). The amount of D_e overdispersion can be calculated for each sample (using the central age model of Galbraith *et al.* 1999), and these estimates are listed in ***Table 4***. Seven of the samples have overdispersion values that range from 5 ± 8 % to 19 ± 1 %, which are similar to the values of 10–20 % commonly reported for quartz grains that had been fully bleached at burial and remained undisturbed thereafter (Jacobs & Roberts 2007). For these samples, the central age model was considered appropriate to calculate the weighted mean D_e values, from which the OSL ages were determined.

The overdispersion value of 32 ± 2 % for AP3 is, however, greater than expected for a fully bleached and undisturbed sample. As sediment grains deposited at Apollo 11 are likely to have been bleached by sunlight for an extended period of time before burial, the most likely cause of the high overdispersion in AP3 is sediment mixing between strata of significantly different age. For this sample, discrete D_e populations can be

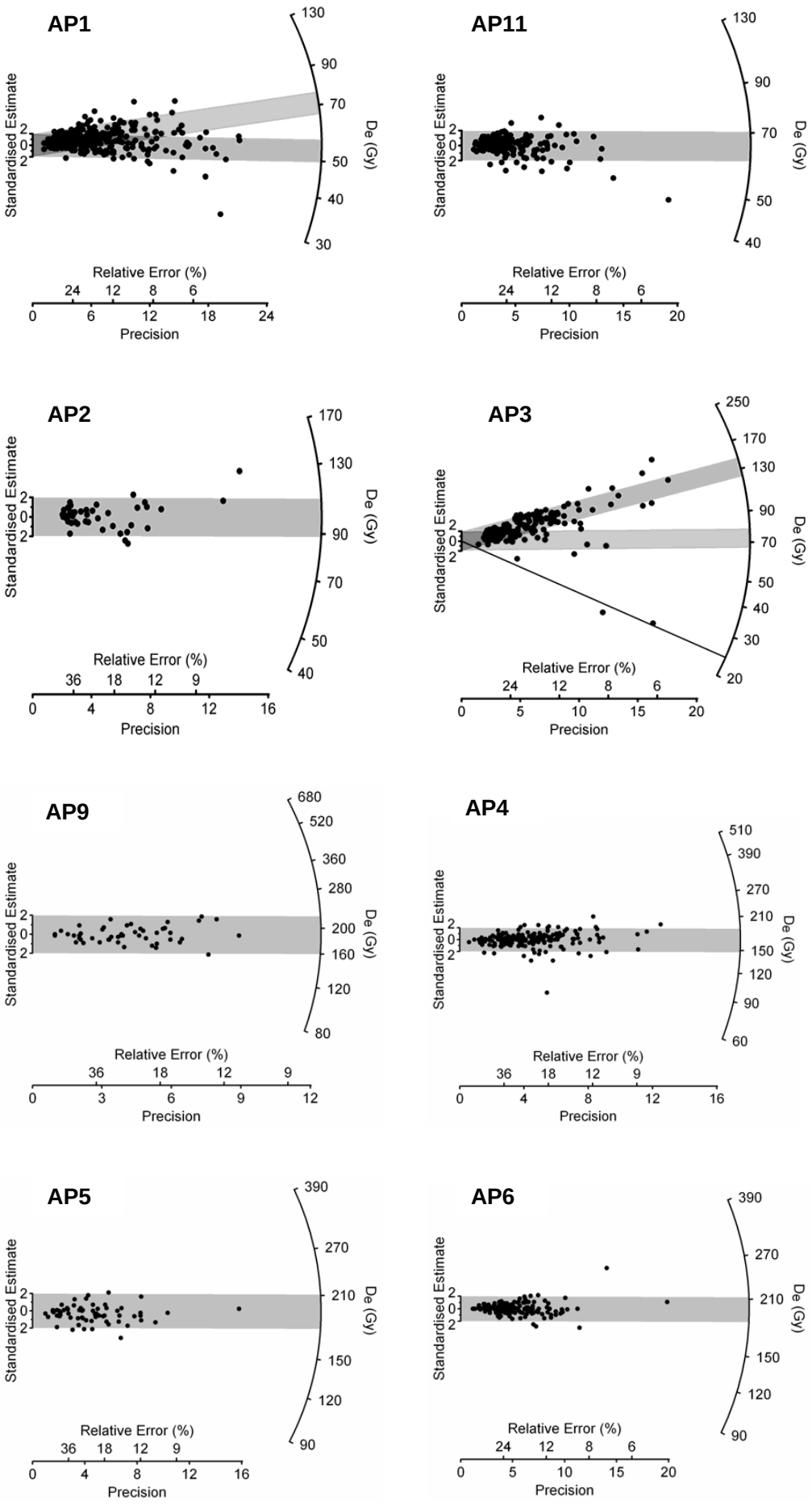

Fig. 14. Radial plots (GALBRAITH 1988) of the equivalent dose (D_e) estimates obtained from individual grains of quartz from each of the Apollo 11 samples.

observed in the radial plot (***Fig. 14***), and the separate age components were distinguished statistically using the finite mixture model (Roberts *et al.* 2000; David *et al.* 2007; Jacobs *et al.* 2008b). The D_e population represented by the vast majority of grains (92 ± 4 %; n = 177) was considered the most appropriate for age determination; the remaining 15 grains that comprise the two smaller D_e components are interpreted as younger, intrusive grains.

The OSL ages for the eight Apollo 11 sediment samples are listed in ***Table 4***, together with the supporting D_e and dose rate data. Uncertainties on the ages are given at 1σ (68 % confidence interval), and are derived by combining in quadrature the uncertainties on the D_e and dose rate estimates. The total uncertainty on the sample D_e was obtained from quadratic addition of the random error (estimated by the particular age model used) and a systematic uncertainty of 2 % (to account for any bias associated with calibration of the laboratory beta source). The total uncertainty on the dose rate for each sample was obtained by summing in quadrature all random errors with the systematic uncertainties associated with estimation of the cosmic-ray dose rate and sample water content.

An age estimate of 71 ± 3 ka (AP6) was obtained for the Still Bay layer and 63 ± 2 ka (AP4) for the Howieson's Poort levels. During the 2007 excavations, a thin, sterile layer was observed between these two complexes and its age was estimated to be 67 ± 3 ka (AP5). These ages were presented in Jacobs *et al.* (2008a): they concur with age estimates for the Still Bay and Howieson's Poort at other sites around southern Africa and with a hiatus of ~7 ka duration between these two industries (Jacobs & Roberts 2008, 2009).

An additional five OSL ages are reported here for samples collected from the late MSA complex at Apollo 11. Two age estimates of 58 ± 3 ka (AP9) and 57 ± 3 ka (AP3) were obtained for deposits near the bottom of this complex: these ages are consistent with the start of the post-Howieson's Poort elsewhere in southern Africa (Jacobs *et al.* 2008a). Samples from the middle and top of the late MSA complex gave ages of 43 ± 3 ka (AP2) and 29.4 ± 1.4 ka (AP11), respectively. These estimates agree with two of the phases identified within this complex by ^{14}C dating, which gave weighted mean ages of 42.8 ± 0.4 cal ka BP for late MSA III and 29.8 ± 1.1 cal ka BP for late MSA I. A pulse of intermediate age (weighted mean: 37.3 ± 0.8 cal ka BP) for the intervening late MSA II was also suggested by ^{14}C dating. Grains of this age are present in the OSL data sets for AP2 and AP11, but they cannot be resolved as a discrete age component owing to the D_e estimates being too imprecise.

Overall, the OSL ages for the MSA levels at Apollo 11 exhibit good stratigraphic consistency, are in agreement with the independent age control at this site (***Table 2*** and ***3***) and elsewhere (Jacobs *et al.* 2008a), and suggest that the MSA deposits accumulated in a series of occupation pulses over an interval of at least 40 millennia from ~71 ka to ~29 ka ago. We were unable to obtain age estimates for the MSA deposits pre-dating the Still Bay, due to these samples having relatively high dose rates (> 3 Gy/ka) and OSL signals that were saturated relative to the absorbed dose.

One of the questions that we hoped the single-grain OSL study would answer was whether the conventional ^{14}C ages for the earliest LSA (weighted mean: 22.3 ± 0.4 cal ka BP) were accurate or too old. The latter could arise due to post-depositional mixing of organic material from the uppermost MSA into the lowermost LSA, coupled with the need to combine several such fragments from an entire excavation spit to generate a sufficient mass of sample for conventional ^{14}C dating. OSL dating of individual grains from sample AP1 offered a means, therefore, of assessing the stratigraphic integrity and age of the lowermost LSA (early LSA II).

Using the central age model estimate of D_e and the dose rate presented in ***Table 4***, an OSL age of 27.6 ± 1.3 ka was obtained for AP1. This age is significantly older than all eight ^{14}C ages for the early LSA II. The D_e overdispersion value for this sample (19 ± 1 %) falls just inside the empirical cut-off value of 20 %, below which the central age model is commonly used to determine the sample D_e (Jacobs & Roberts 2007). The distribution of points in the radial plot exhibited structure, however, suggestive of this sample not being composed of a single population of fully bleached grains that have remained undisturbed since burial. Accordingly, we applied the finite mixture model to the D_e data set for this sample. The optimum statistical fit was a two-component mixture (***Fig. 14***), with each D_e component being overdispersed by 14 %; this value is similar to that measured for the underlying MSA samples that we think consist of single-component D_e distributions.

The lower D_e component of sample AP1 represents 32 % of the grains and corresponds to an age of 22.6 ± 1.3 ka, which is consistent with the conventional ^{14}C ages for early LSA II. The higher D_e component contains the remaining 68 % of the grains and has an age of 30.1 ± 1.6 ka, which is compatible with the conventional and AMS ^{14}C ages for late MSA I. (These OSL age determinations are facilitated by the fact that the dose rates for the earliest LSA and latest MSA deposits are statistically indistinguishable.) Also, a few grains in AP1 have ages consistent with the ^{14}C ages of ~16 cal ka BP obtained on

individual pieces of charcoal collected from early LSA I. These results suggest that the earliest LSA deposits contain mixed-age materials, both sedimentary and organic, with three identified components dating to ~16, ~22 and ~30 ka. Such an admixture was probably due to scuffage of the rockshelter deposits by humans or animals, so the antiquity of the early LSA II artefacts can be constrained only to between ~16 and ~30 ka.

By contrast, the latest MSA shows scant evidence for mixing. Of the 198 grains from AP11 for which D_e values were obtained, only three high-precision estimates (*i.e.*, relative errors on the D_e smaller than 10 %) have ages as young as 20–22 ka. Furthermore, as the overdispersion of 14 ± 2 % determined for AP11 is typical of samples that are known to have been fully bleached at the time of deposition (Jacobs & Roberts 2007), these three estimates most likely form part of the general D_e distribution. Consequently, we consider the painted slabs to be reliably dated to ~ 30 ka, with the underlying deposits recording a series of punctuated occupations during the earlier MSA.

Subsistence and environment

Faunal analysis

In total, about 4500 animal remains (weighing almost 2 kg) from the new excavations at Apollo 11 were available for study. This sample is much smaller than that studied by Thackeray (1979), which consisted of over 20,000 remains. Nevertheless, the results of his and our studies are very similar (see below). From the new animal remains excavated at Apollo 11, a selection of about 60 teeth was taken for purposes of ESR dating, following their taxonomic identification by Joris Peters of the Institut für Paläoanatomie und Geschichte der Tiermedizin at the Ludwig-Maximilians-Universität in München. The remaining faunal material was taken to Belgium and identified there with the aid of reference collections of recent skeletons in the Royal Belgium Institute of Natural Sciences and the Royal Museum for Central Africa. ***Table 6*** summarises the animal taxa recorded by cultural unit in Apollo 11. Although the emphasis in this publication is on the MSA, the remains from the younger levels have also been included for comparison. Fewer than 300 of the remains could be identified to order level or better, mainly because of their high degree of fragmentation.

Many of the animal remains from Apollo 11 are not anthropogenic in origin. At archaeological sites, animals such as small gastropods, snakes, small lizards, small passerine birds and small rodents are usually considered as intrusive, in the absence of any indications to the contrary (*cf.* Gautier 1987). These animals lived and died at the site independently from the human occupants, either contemporaneously or later. Small rodents often gnaw bones to sharpen their ever-growing teeth and their gnawing marks are evident on three bones. Some of the hyrax bones may also have accumulated as a consequence of natural deaths in situ. In cave contexts, the remains of carnivores, such as hyena and leopard, are also not unlikely to be of animals that lived there and died naturally. Moreover, carnivores may also have carried in remains of other animals. This could, for example, explain the presence of animal bones in levels lacking evidence of human settlement. Three cases of carnivore gnawing, two from levels not associated with human occupation, and one case of etching were recorded. In addition, two finds were made in the early MSA levels of what appear to be carnivore faeces. The shape, size, white colour, and the absence of bone remains inside the coprolites are consistent with hyaena faeces (*cf.* Walker 1981). Overall, however, there are relatively few indications that carnivores were present, and their contribution to the accumulated deposits at Apollo 11 is probably small. The large number of ungulate remains compared to carnivore remains in the bone sample further supports this interpretation (*cf.* Klein 1975).

In contrast to the small animals discussed above, remains of tortoise, most hyrax, hare, all bovids and zebra should probably be considered as human food refuse. The ostrich eggshell fragments also have an anthropogenic origin, presumably mostly refuse from the activities of artisans. In the MSA layers, they may represent fragments of flasks (see section "Late MSA previously Apollo 11 MSA 4 [Vogelsang 1998]").

Some of the animal remains have been burned, especially those from the LSA levels, where 10–34 % of the bones show signs of burning. The burned bones usually have a black or grey-black colour, indicating they were heated to temperatures of 500–700°C, which can be reached in a simple camp fire (Lyman 1994: 384–392). In the MSA levels, no more than 5 % of the bones are burned, and almost no evidence of burning was found in the earliest MSA levels. It was not possible to distinguish between bones burned deliberately during food preparation and bones burned accidentally. The high fragmentation of the bones may also be due to human actions, in particular the crushing of bone for marrow extraction. No butchery marks were found on any of the bones, nor were bone artefacts recognised.

The animal taxa identified among the newly excavated bones from Apollo 11 are very similar to those found by Thackeray (1979). Fewer species were recorded in the present study, owing to the smaller sample

	LSA with pottery	Wilton	Early LSA	Late MSA I	Late MSA II & III	Howieson's Poort	Settlement gap	Still Bay	Settlement gap	Early MSA I	Early MSA II	**Total all**
Planorbidae	-	-	1	-	-	-	-	1	-	-	4	**6**
Unidentified gastropod	-	-	-	1	2	1	-	-	1	-	-	**5**
Unidentified mollusc	-	-	-	-	-	-	-	2	-	-	5	**7**
Snake	-	-	-	-	-	2	-	-	-	-	-	**2**
Agama (*Agama* sp.)	-	-	-	1	-	-	-	-	-	-	-	**1**
Small lizard	-	-	-		1	-	-	-	-	-	-	**1**
Tortoise	-	1	1	1	-	1	-	2	-	-	2	**8**
Small passerine bird (Passeriformes)	-	-	-	-	1	-	-	-	-	-	-	**1**
Mouse/rat 1 (*Saccostomus campestris*)	-	-	-	-	1	-	-	-	-	-	-	**1**
Mouse/rat 2 (*Aethomys chrysophilus*)	-	-	-	1	-	-	-	-	-	-	-	**1**
Mouse/rat 3 (*Aethomys namaquensis*)	-	1	-	-	-	-	-	-	-	-	-	**1**
Small rodent	-	-	-	14	13	3	-	-	-	-	-	**30**
Rock hyrax (*Procavia* sp.)	5	6	10	11	4	2	3	3	-	-	2	**46**
Hare, prob. mainly *Lepus* sp.	1	2	8	8	8	3	-	2	-	-	-	**32**
Caracal (*Felis caracal*)	-	-	-	-	1	-	-	-	-	-	-	**1**
Genet (Viverridae) or mongoose (Herpestidae)	-	-	-	-	-	2	-	-	-	-	-	**2**
Small carnivore	-	-	-	-	-	1	-	-	-	-	-	**1**
Warthog (*Phacochoerus* sp.)	-	-	-	1	1	-	-	-	-	-	-	**2**
Small antelope, prob. mainly klipspringer (*Oreotragus oreotragus*)	-	-	1	2	6	8	4	2	-	1	4	**28**
Medium antelope, prob. mainly springbok (*Antidorcas marsupialis*)	-	1	-	1	3	1	1	2	-	-	-	**9**
Small or medium antelope	1	2	6	2	7	3	1	10	-	-	-	**32**
Large antelope	-	-	-	2	-	2	-	-	-	1	-	**5**
Zebra, prob. mainly *Equus zebra*	-	1	3	5	4	5	-	2	-	-	9	**29**
Large antelope or zebra	1	-	2	5	1	1	-	6	-	1	11	**28**
Unidentified bones	158	175	736	159	214	227	68	442	34	99	1788	**4100**
Total numbers of bones	**166**	**189**	**768**	**214**	**267**	**262**	**77**	**474**	**35**	**102**	**1825**	**4379**
Total weight bones (g)	**118**	**108**	**543**	**200**	**162**	**146**	**26**	**247**	**26**	**26**	**397**	**1997**
% Unidentified of all bones	95	93	96	74	80	87	88	93	97	97	98	**94**
Herbivore dropping	2	-	-	-	-	-	-	-	-	-	-	**2**
Small rodent gnawing markings on identified bones	-	1	-	-	1	-	-	1	-	-	-	**3**
Carnivore gnawing marks on identified bones	-	1	-	-	2	-	-	-	-	-	-	**3**
Carnivore etching on identified bones	-	-	-	-	-	1	-	-	-	-	-	**1**
Carnivore dropping	-	-	-	-	-	-	-	-	-	-	2	**2**
% Burned of all bones	17	34	10	4	1	1	3	5	3	0	0	**5**

Tab. 6. List of animal remains and traces by unit of the newly excavated deposits at Apollo 11. Numbers of identified specimens (NISP), unless otherwise indicated.

size. Domestic animals are entirely absent from the collection. The most common remains are of rock hyrax, followed by hare and zebra. Antelopes are also common and are represented by at least two species: klipspringer and springbok. A larger species of antelope is probably also present, but could not be identified more precisely. Warthog forms a minor faunal element. Among the carnivores, remains were found of caracal and a small genet or mongoose. All of these mammals can still be found near the site today. These taxa indicate that hunting took place on the plains (springbok) but mainly in rocky hills (rock hyrax, zebra, klipspringer) (*cf.* Estes 1997). Long bones of the mammals commonly have the articulations not yet fused to the diaphysis, and many of the teeth are deciduous. These observations indicate a predominance of subadult animals, which may have been easier to capture than adult individuals. Several tortoise bones were present. Thackeray (1979) also recorded a fish bone and marine shells, but these were absent from the new sample. The former probably indicates contact with the Orange River, while the latter implies visits to the coast. In the new sample from Apollo 11, some freshwater gastropods of the Planorbidae family were found. These snails, which were not mentioned by Thackeray (1979), can be found mainly in seasonal water basins (Brown 2008). Other intrusive fauna that may provide indications of former environments are the small rodents, but the three species represented in the new collection

	LSA with pottery	Wilton	Early LSA	Late MSA	Howieson's Poort	Still Bay	Early MSA	**Total all**
Tortoise	0	8	3	3	4	7	7	**4**
Rock hyrax (*Procavia* sp.)	63	46	32	29	8	10	7	**21**
Hare, prob. mainly *Lepus* sp.	13	15	26	21	12	7	0	**13**
Warthog (*Phacochoerus* sp.)	0	0	0	3	0	0	0	**1**
Small antelope, prob. mainly klipspringer (*Oreotragus oreotragus*)	0	0	3	5	31	7	14	**15**
Medium antelope, prob. mainly springbok (*Antidorcas marsupialis*)	0	8	0	3	4	7	0	**3**
Small or medium antelope	13	15	19	5	12	34	0	**13**
Large antelope	0	0	0	5	8	0	0	**2**
Zebra, prob. mainly *Equus zebra*	0	8	10	13	19	7	32	**14**
Large antelope or zebra	13	0	6	13	4	21	39	**14**
n	8	13	31	37	26	29	28	**172**

Tab. 7. Relative abundance (%) of consumed animals by cultural unit of the newly excavated deposits at Apollo 11.

from Apollo 11 (*Saccostomus campestris*, *Aethomys chrysophilus* and *Aethomys namaquensis*) occur in a wide range of habitats (IUCN 2009).

Similar species are present in all cultural levels, but the proportions in which they occur varies. Some trends can be seen when only the consumed animals are considered (***Tab. 7***); it should be borne in mind, however, that these trends may not always be significant, owing to the low number of identified bones in each level. Nevertheless, it is clear that rock hyrax occurs in high proportion only in the LSA and late MSA levels. Klipspringer is mainly found in the Howieson's Poort level and, to a lesser extent, in the early MSA units. The species composition of the earliest MSA differs from the other levels in that no hare was found and only few rock hyraxes, but more zebra. The fluctuations in the faunal composition noticed in the new sample from Apollo 11 were not seen by Thackeray (1979). This is probably because his subdivision of cultural levels was not as fine as could be achieved here, owing to the more detailed excavation strategy employed in 2007. It is not clear whether these fluctuations can be explained by ecological changes and/or by human behaviour. In either case, the faunal composition does not seem to record the cooler conditions in the late MSA and early LSA inferred from charcoal analysis (see next section).

Charcoal analysis

Only a restricted amount of palaeoecological information can be gleaned from the analysis of charcoal from Apollo 11, owing to the small size of the samples and uncertainties in the stratigraphy of the terminal Pleistocene layers (specifically, the identification of mixed-age material in the early LSA; see section "D_e distributions and OSL ages"). Nevertheless, some general inferences can be drawn about the history of vegetation and climate in the study area. Such insights are valuable because terrestrial palaeobotanical and archaeobotanical data in Namibia are generally scarce, especially records that extend into the Pleistocene (Eichhorn 2002; Scott *et al.* 2004). Palaeoecological data from marine cores are available for the period in question (Shi & Dupont 1997; Shi *et al.* 1998, 2000), but these may be of limited interpretative value due to possible long-distance transport of pollen grains by ocean currents (Scott *et al.* 2004).

The results of charcoal analysis of the Holocene deposits at Apollo 11 (*i.e.*, LSA with pottery, and Wilton layers) indicate a woody vegetation similar to that of the present day (***Tab. 8***). The most important taxa (*Acacia* type, *Ficus*, *Rhus* and *Grewia* type *tenax*) occur mainly in rock crevices or in the dry river bed of the Nuob Rivier.

The charcoal assemblages for the terminal Pleistocene and Pleistocene/Holocene transition (*i.e.*, the late MSA and early LSA layers, which encompass the Last Glacial Maximum, LGM) differ distinctly from the Holocene assemblages, and are characterised by the presence of *Olea* type. This wood anatomical type most probably represents the species *Olea europaea* ssp. *africana*, which is widespread in southern Africa today; the main exceptions are the Kalahari, the Namib, and large distribution gaps in northern South Africa and in southern and northern Namibia (Coates Palgrave 2002: 918–919). In Namibia, *Olea europaea* ssp. *africana* is common in the eastern Karstveld and occurs in

	LSA with pottery	Wilton	Early LSA	Late MSA I	Late MSA II & III	Howieson's Poort	settlement gap	Still Bay	settlement gap	Early MSA I	Early MSA II
Acacia type	3	5	2			37	17	18		1	
Rhus sp.	1	12	8	1		1		5			cf. 1
Ficus sp.	8	1		12			1	3			
Diospyros/Euclea	2					8	1	11	2		
Maerua/Boscia						4	3	7			
Ziziphus mucronata	1	5					2				
Olea type			36	2		cf. 2		3			
Tarchonanthus type			1				1	22	23	7	2
Chenopodiaceae, *Salsola* type		1	2	5	17	7		2			
Grewia type *tenax*	1	7	18			2		11			
Gymnosporia sp.			1								
Rubiaceae			1								
Rhigozum/Catophractes	5					1	2				
Ehretia sp.		1									
Lycium sp.			1	3		1		4			
Acanthaceae	4					5					
Ozoroa sp.							5	1			
Pappea capensis								3			
Asteraceae undiff.			3								
Aizoaceae, *Tribulocarpus* type				1							
Curroria decidua						1					
monocot			1								
indet		4	6	4	1	3	3			2	

Tab. 8. Charcoal analysis. Identified plant taxa by cultural phase from square Z8 (absolute numbers of charcoal fragments).

dry river beds of the central highlands. There are some scattered localities in the southwest of Namibia, but it has not been recorded in the vicinity of Apollo 11 today (Curtis & Mannheimer 2005: 528–529). *Olea europaea* ssp. *africana* is considered as a slowly growing species that is tolerant to both frost and drought. Scott *et al.* (2004) recorded high values of *Olea* pollen during the LGM in palynological records from the Brandberg, where it occurs in association with other taxa typical of dwarf shrubland, which was widespread during this period. The dwarf shrubland taxa imply cool LGM conditions, and the co-occurrence of *Olea*, *Artemisia* and fern pollen is interpreted as indicating moister conditions. The latter does not necessarily require higher precipitation, only reduced evapotranspiration (Scott *et al.* 2004). The Brandberg massif is a high-mountain area and cooling at the LGM may have influenced woody vegetation more severely than in lower-lying areas, such as the foreland of the Huns Mountains. This may explain the lesser importance of dwarf shrub taxa at Apollo 11 during this period, in addition to the fact that such plants do not yield much fuel and may, therefore, be under-represented in the archaeological deposits due to human choices. Cooler conditions than today at the Pleistocene/Holocene transition have also been inferred from analysis of charcoal in the Kunene Region of northwest Namibia (Eichhorn 2002). This may also explain the replacement of less frost-tolerant tree species by *Olea* in the vicinity of Apollo 11, but provides no insights into the moisture regime.

A small sample of charcoal is available for the period between ~58 and ~43 cal ka BP (*i.e.*, the settlement hiatus between the post-Howieson's Poort and late MSA III layers). This sample contained charcoal only of Chenopodiaceae (*Salsola* type), which is indicative of arid conditions during that interval.

According to the charcoal analysis, the period between ~70 and ~63 cal ka BP (*i.e.*, the Still Bay and Howieson's Poort layers, and the intervening settlement gap) was characterised by diverse woody vegetation, indicating temperature and moisture conditions similar to, or slightly more favourable than, the present. Among these samples, the charcoal assemblage associated with the Still Bay is distinctive, exhibiting the strong presence of Asteraceae (*Tarchonanthus* type). The latter completely dominates the underlying, early MSA layers, which yielded only small samples of charcoal.

Late Pleistocene climate and environment

Today, the site of Apollo 11 is situated in a small region between the two primary rainfall zones in southern Africa (namely the summer and winter rainfall zones),

and can receive precipitation in both winter and summer. Past climatic changes in this region are thought to have been substantially influenced by fluctuations in the north/south migration of the westerlies (Chase & Meadows 2007: 108–110). Unfortunately, terrestrial sedimentary archives are rare for the period of interest, and the preservation conditions of organic materials, such as pollen, are poor due to the arid to semi-arid climate (Scott 1996; Brook *et al.* 1998).

Reconstructions of the palaeoenvironmental conditions in this region have been based mainly, therefore, on evidence from marine cores collected off the Namibian coast (Shi *et al.* 2000, 2001; Stuut *et al.* 2002; Dupont & Wyputta 2003). Detailed regional and local environmental changes cannot be reliably inferred from these records (Chase & Meadows 2007: 112–120), but — at a supra-regional scale — pollen evidence (Shi *et al.* 1998, 2001) and grain-size variations (Stuut *et al.* 2002) indicate increased aridity along the coast of Namibia during MIS 5. The subsequent two marine isotope stages (MIS 4 and MIS 3), which span the period from 75 to 30 ka, witnessed a significant decline in temperature and increased trade winds (*e.g.*, Kirst *et al.* 1999; Stuut *et al.* 2002). The transition between MIS 3 and MIS 2 was marked by a peak in humidity, and was followed by a gradual decrease in precipitation and temperature during the LGM.

Data from terrestrial archives in Namibia are completely absent for MIS 5 and MIS 4, with records only beginning in late MIS 3. Calcified reed beds and lacustrine deposits indicate that the central Namib Desert was more humid then than it is today (Gobabeb: Vogel & Visser 1981; Koichab Pan: Lancaster 1984; Khommabes: Teller & Lancaster 1986a; Narrabeb: Teller & Lancaster 1986b). This reconstruction is supported by the frequency distribution of ^{14}C ages for the Namib Desert, interpreted as humidity indicators by Lancaster (2002), and by the analysis of excess air and oxygen isotopes from the Stampriet Aquifer, which indicated a precipitation peak between 38 and 24 cal ka BP (Stute & Talma 1998). Additional evidence for a late MIS 3 humid phase is found further east, from stromatolites at Klein Awas Pan (Heine 1982) and spring tufas at Aminius Pan and Otjimaruru Pan (Lancaster 1986). Pollen samples from rock hyrax middens in the Brandberg also point to increased relative humidity at 35 and 21 cal ka BP (Scott *et al.* 2004).

At the site of Apollo 11, analysis of the faunal remains from the 1968 and 1972 excavations revealed few taxonomic differences between the various MSA and LSA assemblages (Thackeray 1979). This was interpreted as evidence for generally similar environmental conditions during all settlement phases. All species represented in the Apollo 11 collections (with the exception of equids) occur in the region today and are adapted to arid conditions. Only the high "mean ungulate body-mass" index of the early LSA assemblage hints of higher precipitation in the terminal Pleistocene (Thackeray 1979: 25). Declining abundance of grassland, due to decreasing precipitation, may have been responsible for the disappearance of *Equus capensis* from the Apollo 11 assemblage around 14 cal ka BP. But improved hunting technology may also have contributed to extinctions of game, perhaps after their numbers had been reduced by environmental pressures (Klein 1984: 562).

The analysis of ^{13}C values for zebra teeth showed that the ratio of C_3 to C_4 plants did not change significantly between glacial and interglacial periods, indicating environmental conditions similar to the present ones, with no significant northward extension of winter rainfall (Vogel 1983; Van Zinderen Bakker 1984).

Analysis of the newly-excavated bones from Apollo 11 broadly confirms these results. The proportions of different species recognised in the faunal assemblage exhibits more variation than described previously for the various cultural layers, but it is not clear whether these fluctuations reflect changes in ecology and/or human behaviour, or are a consequence of the small sample sizes.

The charcoal analysis yielded more informative results in this respect. The Holocene layers are characterised by a woody vegetation similar to that at present, whereas the occurrence of the frost-tolerant taxon *Olea* indicates cooler climatic conditions during the late MSA/early LSA. However, it is not possible to draw direct conclusions on the moisture regime from these data. Conditions more arid than today are inferred for the time gap in settlement between the post-Howieson's Poort and the late MSA III (58–43 ka), based on the recovery of charcoal only of Chenopodiaceae from this thin layer. Both the Howieson's Poort and Still Bay layers are characterised by diverse woody vegetation, which implies temperature and moisture conditions similar to those existing today. The environmental significance of predominantly Asteraceae (*Tarchonanthus* type) charcoal in the early MSA layers is not clear, as this type includes species with a very wide ecological range.

The results of the faunal and charcoal analyses mainly pertain to environmental conditions during settlement periods, whereas changes in the character of the sediments may also be informative of climatic changes during times of site abandonment. Climatic conditions

more humid than today are inferred for the basal sediment layers, which are highly interspersed with fine-grained rockfall. From sediment unit T upwards, the quantity of rockfall decreases and natural processes of sedimentation become increasingly subordinate to human activities as agents of accumulation of the Apollo 11 deposit. The decreased contribution of sediments to the Still Bay and Howieson's Poort layers by natural processes may indicate increasing aridification during these periods of settlement, with the climatic conditions being similar to present. Thin layers of silty sediment and/or very fine rock debris coincide with gaps in settlement, as suggested by very low artefact densities, and might be associated with increased aeolian sedimentation under extremely arid conditions. The most prominent of these layers is sediment unit S, which separates the Still Bay from the Howieson's Poort and is dated to 67 ± 3 ka. Sediment unit M, which marks the transition between the latest MSA and earliest LSA, represents the last major event of weathering and dissolution of the shelter roof. Since that time, conditions appear to have been similar to the present day, except for minor climatic variations.

In conclusion, environmental conditions during most settlement phases at Apollo 11 seem to have been similar to those prevailing today. Only during the earliest MSA settlement phases preserved in the basal deposits (which are still undated) might conditions have been more humid than at present. Settlement gaps appear to coincide with the most arid periods, but a clear correlation with supra-regional climatic changes is not yet possible.

Concluding remarks

Apollo 11 is one of the archaeological flagship sites in southern Africa, boasting one of the most complete archaeological sequences with all important cultural units known from the regional MSA and LSA. Especially for the Middle Stone Age period such long-sequence sites are still few in the whole region. An inter-regional comparison of these key sequences is hindered by the low number of retouched stone tools and the absence of a widely recognised classification scheme for MSA type forms. Technologically based analysis, such as the reconstruction of the châines opératoires (*e.g.*, Wurz 2002; Rigaud *et al.* 2006; Soriano *et al.* 2007) are still the exception, but might be a way to improve MSA classification schemes. However, at least the Apollo 11 inventories show only limited technological variability during the MSA. Keeping these restrictions in mind, the Apollo 11 cultural complexes correspond to the general sequence of the southern African Middle Stone Age, as described by Volman (1984). Certainly, his fourfold scheme, as much as the previous classification of the Apollo 11 assemblage (Vogelsang 1998), offers only a very rough subdivision. For Apollo 11, our small re-excavation has demonstrated the potential of the site to produce a refined differentiation of the MSA material, provided suitable excavation methods are used.

Apollo 11 is also one of the most comprehensively dated sites in the region. However, the conventional ^{14}C measurements of composite samples from the original excavation entailed the risk of dating mixed-aged materials. The checking of the validity of the conventional ^{14}C ages for the late MSA and early LSA levels by AMS measurements confirmed the previous ages for the early LSA I, but not for the early LSA II. For the late MSA levels three occupation phases can be distinguished at ~30, ~37 and ~43 cal ka BP, respectively. This underlines the need to differentiate the cultural material of the late MSA by future excavations and analysis.

In view of the possibility of mixing in the lowermost LSA levels, and the obtainment of infinite ^{14}C ages for the deposits underlying the late MSA complex, single-grain OSL dating of the sediments at Apollo 11 was carried out. Overall, the OSL ages for the MSA levels at Apollo 11 exhibit good stratigraphic consistency, are in agreement with the independent age control at this site and elsewhere (Jacobs *et al.* 2008a), and suggest that the MSA deposits accumulated in a series of occupation pulses over an interval of at least 40 millennia from ~71 ka to ~29 ka ago. Our results suggest that the earliest LSA deposits contain mixed-age materials, so the antiquity of the early LSA II artefacts can be constrained only to between ~16 and ~30 ka. Samples from the middle and top of the late MSA complex gave ages of 43 ± 3 ka and 29.4 ± 1.4 ka, respectively and correspond to ^{14}C ages for the late MSA I and late MSA III. Consequently, we consider the painted slabs that were found in late MSA I deposits to be reliably dated to ~ 30 ka. At the bottom of the late MSA levels age estimates of 58 ± 3 ka and 57 ± 3 ka are consistent with the start of the post-Howieson's Poort elsewhere in southern Africa (Wadley & Jacobs 2006; Jacobs *et al.* 2008a).

An age estimate of 71 ± 3 ka was obtained for the Still Bay layer and 63 ± 2 ka for the Howieson's Poort layer, which were separated by a thin, sterile layer with an age of 67 ± 3 ka. These ages concur with age estimates for the Still Bay and Howieson's Poort at other sites around southern Africa and with a hiatus of ~7 ka duration between these two industries (Jacobs & Roberts 2008, 2009). It was not possible to obtain age estimates for the MSA deposits pre-dating the Still Bay.

The results of our small re-excavation underline the importance of Apollo 11 for the understanding of the Middle Stone Age period in southern Africa. All the more shocking were the conditions of the site at the start of our fieldwork in 2007: the refill of the old excavation trench had been severely vandalised. Fortunately, no unexcavated archaeological deposits had been affected, but this incident illustrates the potential risk of serious damage to the site. Regardless of the motivation for its destruction, whether by vandals or treasure hunters, action should be implemented to protect this heritage site of worldwide archaeological significance.

Acknowledgements

The project "Feinchronologische Differenzierung und absolutchronologische Datierung der Middle-Stone-Age-Schichten der Höhle Apollo 11 in Namibia" was funded by the Deutsche Forschungsgemeinschaft (RI 936/4). Fieldwork was supported by a grant of the "Jutta Vogel Stiftung" and by the Australian Research Council, which also funded the OSL dating through Discovery Project grant DP0666084. We are grateful to all members of the National Heritage Council and the State Museum of Namibia for friendly support and for granting the necessary research permits. Wim Wendelen (Royal Belgian Museum for Central Africa) helped with the identifications of the small rodent remains, and Thierry Backeljau (Royal Belgian Institute of Natural Sciences) assisted with those of the Planorbidae. Wim Van Neer (Royal Belgian Institute of Natural Sciences) and Sarah Wurz (Institute of Prehistoric Archaeology, University of Cologne) are acknowledged for their comments on an early draft of this manuscript.

References

Aitken, M.J. 1985. *Thermoluminescence Dating*. Academic Press, London.

Aitken, M.J. 1998. *An Introduction to Optical Dating: The Dating of Quaternary Sediments by the Use of Photon-stimulated Luminescence*. Oxford University Press, Oxford.

Backwell, L., d'Errico, F. & Wadley, L. 2008. Middle Stone Age bone tools from the Howiesons Poort layers, Sibudu Cave, South Africa. *Journal of Archaeological Science* 35 (6), 1566–1580.

Bøtter-Jensen, L., McKeever, S.W.S., Wintle, A.G. 2003. *Optically Stimulated Luminescence Dosimetry*. Elsevier, Amsterdam.

Bøtter-Jensen, L. & Mejdahl, V. 1988. Assessment of beta dose-rate using a GM multicounter system. *Nuclear Tracks and Radiation Measurements* 14, 187–191.

Brook, G.A., Cowart, J.B. & Brandt, S.A. 1998. Comparison of Quaternary environmental change in eastern and southern Africa using cave speleothem, tufa and rock shelter sediment data. In: Alsharhan, A.S., Glennie, K.W., Whittle, G.L. & Kendall, C.G.S.C. (eds.) 1998, *Quaternary Deserts and Climatic Change*. Balkema, Rotterdam, pp. 239–249.

Brown, D. 2008. *Freshwater Snails of Africa and Their Medicinal Importance* (revised 2nd edition). Taylor and Francis, London.

Chase, B.M. & Meadows, M.E. 2007. Late Quaternary dynamics of southern Africa's winter rainfall zone. *Earth-Science Reviews* 84, 103–138.

Coates Palgrave, K.C. 2002. *Trees of Southern Africa* (3rd edition, revised and updated by M. Coates Palgrave). Struik Publishers, Cape Town.

Curtis, B. & Mannheimer, C. 2005. *Tree Atlas of Namibia*. National Botanical Research Institute, Windhoek.

David, B., Roberts, R.G., Magee, J., Mialanes, J., Turney, C., Bird, M., White, C., Fifield, L.K. & Tibby, J. 2007. Sediment mixing at Nonda Rock: investigations of stratigraphic integrity at an early archaeological site in northern Australia and implications for the human colonisation of the continent. *Journal of Quaternary Science* 22 (5), 449–479.

d'Errico, F. & Henshilwood, C. 2007. Additional evidence for bone technology in the southern African Middle Stone Age. *Journal of Human Evolution* 52 (2), 142–163.

Dupont, L.M. & Wyputta, U. 2003. Reconstructing pathways of aeolian pollen transport to the marine sediments along the coastline of SW Africa. *Quaternary Science Reviews* 22, 157–174.

Eichhorn, B. 2002. *Anthrakologische Untersuchungen zur Vegetationsgeschichte des Kaokolandes, Nordwest-Namibia*. Dissertation, Mathematisch-Naturwissenschaftliche Fakultät der Universität zu Köln. URN (NBN). urn:nbn:de:hbz:38-11784.

Estes, R.D. 1997. *The Behaviour Guide to African Mammals. Including Hoofed Mammals, Carnivores, Primates*. Russel Friedman Books, South Africa.

Freundlich, J.C., Schwabedissen, H. & Wendt, W.E. 1980. Köln radiocarbon measurements II. *Radiocarbon* 22 (1), 68–81.

Galbraith, R.F. 1988. Graphical display of estimates having differing standard errors. *Technometrics* 30 (3), 271–281.

Galbraith, R.F., Roberts, R.G., Laslett, G.M., Yoshida, H. & Olley, J.M. 1999. Optical dating of single and multiple grains of quartz from Jinmium rock shelter, northern Australia: Part I, experimental design and statistical models. *Archaeometry* 41 (2), 339–364.

Gautier, A. 1987. Taphonomic groups: how and why? *Archaeozoologia* 1 (2), 47–52.

Germs, G.J.B. 1972. The stratigraphy and paleontology of the lower Nama Group, South West Africa. *Bulletin of the Precambrian Research Unit* 12, 1–250.

Germs, G.J.B. 1983. Implications of a sedimentary facies and depositional environmental analysis of the Nama Group in South West Africa/Namibia. In: Miller, R.M. (ed.), *Evolution of the Damara Orogen of South West Africa/Namibia.* Special Publication of the Geological Society of South Africa 11. Geological Society of South Africa, Johannesburg, pp. 89–114.

Giess, W. 1971. A preliminary vegetation map of South West Africa. *Dinteria* 4, 5–114.

Grotzinger, J., Adams, E.W. & Schröder, S. 2005. Microbial–metazoan reefs of the terminal Proterozoic Nama Group (*c*. 550–543 Ma), Namibia. *Geological Magazine* 142 (5), 499–517.

Heine, K. 1982. The main stages of the late Quaternary evolution of the Kalahari region, southern Africa. *Palaeoecology of Africa* 15, 53–76.

Henderson, Z. 2002. A dated cache of ostrich-eggshell flasks from Thomas' Farm, Northern Cape Province, South Africa. *South African Archaeological Bulletin* 57, 38–40.

Henshilwood, C., d'Errico, F., Marean, C., Milo, R. & Yates, R. 2001. An early bone tool industry from the Middle Stone Age at Blombos Cave, South Africa: implications for the origins of modern human behaviour, symbolism and language. *Journal of Human Evolution* 41 (4), 631–678.

Henshilwood C.S., d'Errico, F., Yates, R., Jacobs, Z., Tribolo, C., Duller, G.A.T., Mercier, N., Sealy, J.C., Valladas, H., Watts, I. & Wintle, A.G. 2002. Emergence of modern human behavior: Middle Stone Age engravings from South Africa. *Science* 295, 1278–1280.

Henshilwood, C.S., d'Errico, F. & Watts, I. 2009. Engraved ochres from the Middle Stone Age levels at Blombos Cave, South Africa. *Journal of Human Evolution* 57 (1), 27–47.

IUCN 2009. IUCN Red List of Threatened Species. Version 2009.2. <www.iucnredlist.org>. Downloaded on 13 November 2009.

Jacobs, Z., Duller, G.A.T. & Wintle, A.G. 2006a. Interpretation of single grain D_e distributions and calculation of D_e. *Radiation Measurements* 41 (3), 264–277.

Jacobs, Z., Duller, G.A.T., Wintle, A.G. & Henshilwood, C.S. 2006b. Extending the chronology of deposits at Blombos Cave, South Africa, back to 140 ka using optical dating of single and multiple grains of quartz. *Journal of Human Evolution* 51 (3), 255–273.

Jacobs, Z., Wintle, A.G. & Duller, G.A.T. 2003. Optical dating of dune sand from Blombos Cave, South Africa: I-multiple grain data. *Journal of Human Evolution* 44 (5), 599–612.

Jacobs, Z. & Roberts, R.G. 2007. Advances in optically stimulated luminescence dating of individual grains of quartz from archeological deposits. *Evolutionary Anthropology* 16 (6), 210–223.

Jacobs, Z. & Roberts, R.G. 2008. Testing times: old and new chronologies for the Howieson's Poort and Still Bay industries in environmental context. *South African Archaeological Society Goodwin Series* 10, 9–34.

Jacobs, Z. & Roberts, R.G. 2009. Human history written in stone and blood. *American Scientist* 97 (4), 302–309.

Jacobs, Z., Roberts, R.G., Galbraith, R.F., Deacon, H.J., Grün, R., Mackay, A., Mitchell, P., Vogelsang, R. & Wadley, L. 2008a. Ages for the Middle Stone Age of southern Africa: implications for human behavior and dispersal. *Science* 322, 733–735.

Jacobs, Z., Wintle, A.G., Roberts, R.G. & Duller, G.A.T. 2008b. Equivalent dose distributions from single grains of quartz at Sibudu, South Africa: context, causes and consequences for optical dating of archaeological deposits. *Journal of Archaeological Science* 35 (7), 1808–1820.

Kandel, A.W. 2004. Modification of ostrich eggs by carnivores and its bearing on the interpretation of archaeological and paleontological finds. *Journal of Archaeological Science* 31 (4), 377–391.

Kirst, G.J., Schneider, R.R., Muller, P.J., von Storch, I. & Wefer, G. 1999. Late Quaternary temperature variability in the Benguela Current System derived from alkenones. *Quaternary Research* 52 (1), 92–103.

Klein, R.G. 1975. Palaeoanthropological implications of the non-archaeological bone assemblage from Swartklip 1, South-Western Cape Province, South Africa. *Quaternary Research* 5 (2), 275–288.

Klein, R.G. 1984. Mammalian extinctions and Stone Age people in Africa. In: Martin, P. S. & Klein, R.G. (eds.), *Quaternary Extinctions: A Prehistoric Revolution*. University of Arizona Press, Tucson, pp. 553–573.

Lancaster, N. 1984. Paleoenvironments in the Tsondab Valley, central Namib Desert. *Palaeoecology of Africa* 16, 411–419.

Lancaster, N. 1986. Pans in the southwestern Kalahari: a preliminary report. *Palaeoecology of Africa* 17, 59–67.

Lancaster, N. 2002. How dry was dry? Late Pleistocene palaeoclimates in the Namib Desert. *Quaternary Science Reviews* 21 (7), 769–782.

Lian, O.B. & Roberts, R.G. 2006. Dating the Quaternary: progress in luminescence dating of sediments. *Quaternary Science Reviews* 25 (19–20), 2449–2468.

Lombard, M. 2006. Direct evidence for the use of ochre in the hafting technology of Middle Stone Age tools from Sibudu Cave. *Southern African Humanities* 18 (1), 57–67.

Lombard, M. 2008. Finding resolution for the Howiesons Poort through the microscope: micro-residue analysis of segments from Sibudu Cave, South Africa. *Journal of Archaeological Science* 35 (1), 26–41.

Lyman, R.L. 1994. *Vertebrate Taphonomy. Cambridge Manuals in Archaeology*. Cambridge University Press, Cambridge.

Mackay, A. & Welz, A. 2008. Engraved ochre from a Middle Stone Age context at Klein Kliphuis in the Western Cape of South Africa. *Journal of Archaeological Science* 35 (6), 1521–1532.

Martin, H. 1965. *The Precambrian Geology of South West Africa and Namaqualand*. Precambrian Research Unit, University of Cape Town, Cape Town.

Mejdahl, V. 1979. Thermoluminescence dating: beta-dose attenuation in quartz grains. *Archaeometry* 21 (1), 61–72.

Mendelsohn, J., Jarvis, A., Roberts, C. & Robertson, T. 2002. *Atlas of Namibia. A Portrait of the Land and its People*. David Philip Publishers, Cape Town.

Mitchell, P. 2002. *The Archaeology of Southern Africa*. Cambridge University Press, Cambridge.

Morris, D. 1994. An ostrich eggshell cache from the Vaalbos National Park, Northern Cape. *South African Field Archaeology* 3, 55–58.

Müller, M.A.N. 1985. *Gräser Südwestafrika/Namibias*. John Meinert Printers, Windhoek.

Prescott, J.R. & Hutton, J.T. 1994. Cosmic ray contributions to dose rates for luminescence and ESR dating: large depths and long-term time variations. *Radiation Measurements* 23 (2–3), 497–500.

Readhead, M.L. 1987. Thermoluminescence dose rate data and dating equations for the case of disequilibrium in the decay series. *Nuclear Tracks and Radiation Measurements* 13 (4), 197–207.

Rigaud, J.-P., Texier, P.-J., Parkington, J. & Poggenpoel, C. 2006. Le mobilier Stillbay et Howiesons Poort de l'abri Diepkloof. La chronologie du Middle Stone Age sud-africain et ses implications. *Palevol* 5 (7), 839–849.

Roberts, R.G., Galbraith, R.F., Yoshida, H., Laslett, G.M. & Olley, J.M. 2000. Distinguishing dose populations in sediment mixtures: a test of single-grain optical dating procedures using mixtures of laboratory-dosed quartz. *Radiation Measurements* 32 (5–6), 459–465.

Scherz, E.R. 1970. *Felsbilder in Südwest Afrika, Teil I: Die Gravierungen in Südwest-Afrika ohne den Nordwesten des Landes*. Fundamenta A7. Böhlau Verlag, Köln/Wien.

Scherz, E.R. 1986. *Felsbilder in Südwest Afrika, Teil III: Die Malereien*. Fundamenta A7/III. Böhlau Verlag, Köln/Wien.

Scott, L. 1996. Palynology of hyrax middens: 2000 years of palaeoenvironmental history in Namibia. *Quaternary International* 33, 73–79.

Scott, L., Marais, E. & Brook, G.A. 2004. Fossil hyrax dung and evidence of Late Pleistocene and Holocene vegetation types in the Namib Desert. *Journal of Quaternary Science* 19 (8), 829–832.

Shi, N. & Dupont, L. 1997. Vegetation and climatic history of southwest Africa: a marine palynological record of the last 300.000 years. *Vegetation History and Archaeobotany* 6 (2), 117–131.

Shi, N., Dupont, L. & Beug, H.-J. 2000. Correlation between vegetation in southwestern Africa and oceanic upwelling in the past 21,000 years. *Quaternary Research* 54 (1), 72–80.

Shi, N., Dupont, L., Beug, H.-J. & Schneider, R. 1998. Vegetation and climate changes during the last 21000 years in S.W. Africa based on a marine pollen record. *Vegetation History and Archaeobotany* 7 (3), 127–140.

Shi, N., Schneider, R., Beug, H.-J. & Dupont, L.M. 2001. Southeast trade wind variations during the last 135 kyr: evidence from pollen spectra in eastern South Atlantic sediments. *Earth and Planetary Science Letters* 187 (3–4), 311–321.

Singer, R. & Wymer, J. 1982. *The Middle Stone Age at Klasies River Mouth in South Africa*. University of Chicago Press, Chicago.

Smith, M.A., Prescott, J.R. & Head, M.J. 1997. Comparison of 14C and luminescence chronologies at Puritjarra rock shelter, central Australia. *Quaternary Science Reviews* 16 (3–5), 299–320.

Soriano, S., Villa, P. & Wadley, L. 2007. Blade technology and tool forms in the Middle Stone Age of South Africa: the Howiesons Poort and post-Howiesons Poort at Rose Cottage Cave. *Journal of Archaeological Science* 34 (5), 681–703.

Stengel, I. & Leser, H. 2004. Late Quaternary valley-fill terraces and palaeoenvironments of the Huns River, southern Namibia. *Die Erde* 135 (2), 129–149.

Stute, M. & Talma, A.S. 1998. Glacial temperatures and moisture transport regimes reconstructed from noble gas and $\delta^{18}O$, Stampriet, aquifer, Namibia. In: *Proceedings of the International Symposium on Isotope Techniques in the Study of Past and Current Environmental Changes in the Hydrosphere and Atmosphere*. IAEA, Wien, p. 307.

Stuut, J.-B.W., Prins, M.A., Schneider, R.R., Weltje, G.J., Jansen, J.H.F. & Postma, G. 2002. A 300 kyr record of aridity and wind strength in southwestern Africa: inferences from grain-size distributions of sediments on Walvis Ridge, SE Atlantic. *Marine Geology* 180 (1–4), 221–233.

Teller, J.T. & Lancaster, N. 1986a. History of sediments at Khommabes, central Namib Desert. *Madoqua* 14 (4), 409–420.

Teller, J.T. & Lancaster, N. 1986b. Lacustrine sediments at at Narabeb in the central Namib desert, Namibia. *Palaeogeography, Palaeoclimatology, Palaeoecology* 56 (3–4), 177–195.

Thackeray, A.I. 1992. The Middle Stone Age south of the Limpopo River. *Journal of World Prehistory* 6 (4), 385–440.

Thackeray, J.F. 1979. An analysis of faunal remains from archaeological sites in southern South West Africa (Namibia). *The South African Archaeological Bulletin* 34 (129), 18–33.

Van Zinderen Bakker, E.M. 1984. Aridity along the Namibian coast. *Palaeoecology of Africa* 16, 149–162.

Villa, P., Soressi, M., Henshilwood, C.S. & Mourre, V. 2009. The Still Bay points of Blombos Cave (South Africa). *Journal of Archaeological Science* 36 (2), 441–460.

Vogel, J.C. 1983. Isotopic evidence for past climates and vegetation of South Africa. *Bothalia* 14, 391–394.

Vogel, J.C. & Visser, E. 1981. Pretoria radiocarbon dates. *Radiocarbon* 23 (1), 43–80.

Vogelsang, R. 1996. The Middle Stone Age in south-western Namibia. In: Pwiti, G. & Soper, R. (eds.), *Aspects of African Archaeology. Papers from the 10th Congress of the Pan African Association for Prehistory and Related Studies*. University of Zimbabwe Publications, Harare, pp. 207–213.

Vogelsang, R. 1998. *Middle-Stone-Age-Fundstellen in Südwest-Namibia*. Africa Praehistorica 11. Heinrich-Barth-Institut, Köln.

Volman, T.P. 1984. Early prehistory of southern Africa. In: Klein, R.G. (ed.), *Southern African Prehistory and Palaeoenvironments*. A.A. Balkema, Rotterdam, pp. 169–220.

Wadley, L. & Jacobs, Z. 2006. Sibudu Cave: background to the excavations, stratigraphy and dating. *Southern African Humanities* 18 (1), 1–26.

Walker, C. 1981. *Signs of the Wild. Field Guide to the Tracks and Signs of the Mammals of Southern Africa*. Natural History Publications, Johannesburg.

Wendt, W.E. 1972. Preliminary report on an archaeological research programme in South West Africa. *Cimbebasia* B (2), 1–61.

Wendt, W.E. 1974. "Art mobilier" aus der Apollo 11-Grotte in Südwest-Afrika. *Acta Praehistorica et Archaeologica* 5, 1–42.

Wendt, W.E. 1976. "Art mobilier" from the Apollo 11 Cave, South West Africa: Africa's oldest dated works of art. *South African Archaeological Bulletin* 31, 5–11.

Weninger, B. & Jöris, O. 2008. A 14C age calibration curve for the last 60 ka: the Greenland-Hulu U/Th timescale and its impact on understanding the Middle to Upper Paleolithic transition in Western Eurasia. *Journal of Human Evolution* 55 (5), 772–781.

White, S., Stollhofen, H., Stanistreet, I.G. & Lorenz, V. 2009. Pleistocene to Recent rejuvenation of the Hebron Fault, SW Namibia. *Geological Society, London, Special Publications* 316, 293–317.

Willoughby, P.R. 2007. *The Evolution of Modern Humans in Africa: A Comprehensive Guide*. AltaMira Press, Lanham.

Wintle, A.G. 2008. Fifty years of luminescence dating. *Archaeometry* 50 (2), 276–312.

Wurz, S. 2002. Variability in the Middle Stone Age lithic sequence, 115,000–60,000 years ago at Klasies River, South Africa. *Journal of Archaeological Science* 29 (9), 1001–1015.